

**Characterization and Properties of Powder Metallurgy Alumina-  
Iron and Alumina-Copper Ceramic Composites**

by

Yew Lih Chi

16580

Dissertation submitted in partial fulfilment of  
the requirements for the  
BACHELOR of ENGINEERING (Hons)  
(MECHANICAL ENGINEERING)

JANUARY 2016

Universiti Teknologi PETRONAS

Bandar Seri Iskandar

31750 Tronoh

Perak Darul Ridzuan

CERTIFICATION OF APPROVAL

**Characterization and Properties of Powder Metallurgy Alumina-Iron and  
Alumina-Copper Ceramic Composites**

by

Yew Lih Chi

16580

A project dissertation submitted to the

Mechanical Engineering Programme

Universiti Teknologi PETRONAS

In partial fulfilment of the requirements for the

BACHELOR of ENGINEERING (Hons)

(MECHANICAL ENGINEERING)

Approved by,

---

(AP Dr. Othman Bin Mamat)

UNIVERSITI TEKNOLOGI PETRONAS

TRONOH, PERAK

Jan 2016

## CERTIFICATION OF ORIGINALITY

This is to certify that I am responsible for the work submitted in this project, that the original work is my own except as specified in the references and acknowledgements, and that the original work contained herein have not been undertaken or done by unspecified sources or persons.

---

(YEW LIH CHI)

## ABSTRACT

Ceramic metal composites are engineered materials that use metals as reinforcements to improve the mechanical properties such as flexural strength and fracture toughness of ceramics. The trend of mechanical properties does not increase or decrease proportionally to the volume of metal reinforcement added. Incorporation of metals to ceramic may enhance the mechanical properties, but over addition of metals after its optimum volume give adverse effect. The objectives of this paper are to study the effects of iron and copper additions in density and flexural strength to the alumina-iron and alumina-copper composites and to determine the optimum volume of iron and copper additions in the alumina composites, respectively. Powder metallurgy was the method used to fabricate alumina matrix composites containing 5 and 10 vol.% of iron or copper additions respectively. The alumina and metal powders are mixed, undergone uniaxial dry pressing with 375MPa and sintering at 1100°C in Nitrogen atmosphere. A total of 25 samples including both alumina matrix composites and pure alumina samples are fabricated. The obtained samples are then characterized for density, undergone three-point bending test and microstructural analysis. The results showed that density of alumina increased significantly with additions of iron and copper to their respective composites. From flexural test results, alumina-iron composites with 10 vol.% iron content achieved the highest flexural strength among all compositions, which is 317.5MPa. From the combined data of microstructural analysis, relative density and flexural strength, the optimum iron content for alumina-iron composite is in the range of 5 vol.% to 10 vol.%, whereas the optimum copper content for alumina-copper composite is at 10 vol.%.

## **ACKNOWLEDGEMENT**

First and foremost, I would like to extend my deepest gratitude to my supervisor, AP. Dr. Othman Bin Mamat for his unlimited guidance, support, motivation and patience throughout the entire project. His knowledge and experience really helped me in completing this project successfully. Without his support, this project would not have been done successfully.

Besides, I would like to express my gratitude to my examiner, Dr. Saeid Kakooei for his feedback and comments for the betterment of this project. I would also like to thank all the technologists from Mechanical Engineering Department for their commitment and guidance. Their help made the sample fabrication and testing process successful.

Last but not least, the acknowledgement also goes to my beloved family and colleagues who showed continuous support and encouragement during the process of project completion.

# TABLE OF CONTENTS

<b>CERTIFICATION OF APPROVAL</b> .....	i
<b>CERTIFICATION OF ORIGINALITY</b> .....	ii
<b>ABSTRACT</b> .....	iii
<b>ACKNOWLEDGEMENT</b> .....	iv
<b>LIST OF FIGURES</b> .....	vii
<b>LIST OF TABLES</b> .....	viii
<b>CHAPTER 1 INTRODUCTION</b> .....	1
1.1 Background of Study .....	1
1.2 Problem Statement .....	2
1.3 Objective .....	2
1.4 Scope of Study.....	3
<b>CHAPTER 2 LITERATURE REVIEW</b> .....	4
2.1 Ceramic-Metal Composites .....	4
2.2 Rule of Mixtures.....	4
2.2 Alumina Powder .....	5
2.3 Iron Powder .....	5
2.4 Copper Powder .....	6
2.5 Powder Metallurgy .....	6
2.6 Microstructures of Composites .....	7
2.7 Green, Sintered and Relative Densities of Composites.....	8
2.8 Mechanical Properties of Composites .....	9
2.8.1 Flexural Test .....	10
<b>CHAPTER 3 METHODOLOGY</b> .....	11
3.1 Research Methodology .....	11
3.2 Project Gantt Chart .....	13
3.3 Key Milestones.....	15
3.4 Experimental Works.....	16
3.4.1 Raw Materials and Equipment.....	16
3.4.2 XRF analysis.....	16
3.4.3 Mixing Process .....	17
3.4.4 Compaction Process.....	18
3.4.5 Sintering Process .....	18
3.4.6 Measurement of Green and Sintered Densities.....	19

3.5 Samples Analysis .....	19
3.5.1 Three-Point Bending Test.....	19
3.5.2 Microstructure.....	19
<b>CHAPTER 4 RESULTS AND DISCUSSION</b> .....	20
4.1 Powders Shape, Concentration and Density.....	20
4.2 Composites Density.....	21
4.3 Flexural Strength of Composites .....	26
4.4 Microstructures of Composites .....	28
4.5 Optimum Volume of Iron or Copper Additions .....	31
<b>CHAPTER 5 CONCLUSION AND RECOMMENDATIONS</b> .....	35
5.1 Conclusion.....	35
5.2 Recommendations .....	35
<b>REFERENCES</b> .....	36
APPENDIX A – Table of engineering alumina grades A1- A9 and their characteristics at room temperature .....	39
APPENDIX B – Equipment needed .....	40
APPENDIX C – Sample calculations for mass of sample.....	42
APPENDIX D1 – Mould design for compaction process.....	43
APPENDIX D2 – Mould dimensions.....	44
APPENDIX E – XRF analysis results for alumina, iron and copper powder.....	45
APPENDIX F – Graph of density against compaction pressure for iron .....	46
APPENDIX G – Sintered samples .....	47
APPENDIX H1 – Mass, volume and density of green compacts .....	49
APPENDIX H2 – Mass, volume and density of sintered samples .....	50

## LIST OF FIGURES

Figure 3.1: Project Flow Chart .....	11
Figure 3.2: Project Gantt Chart (FYP 1) .....	13
Figure 3.3: Project Gantt Chart (FYP 2) .....	14
Figure 3.4: Project Key Milestones .....	15
Figure 3.5: Sintering Cycle .....	18
Figure 4.1: SEM micrographs of (a) Alumina powder, (b) Iron powder, (c) Copper powder, (d) Paraffin wax .....	20
Figure 4.2: Graph of Density against Volume Percentage of Iron .....	23
Figure 4.3: Graph of Density against Volume Percentage of Copper .....	24
Figure 4.4: Graph of Relative Density against Volume Percentage of Iron or Copper .....	25
Figure 4.5: Graph of Flexural Strength against Volume Percentage of Metals .....	27
Figure 4.6: SEM micrographs of (a) 100% Al <sub>2</sub> O <sub>3</sub> , (b) 95% Al <sub>2</sub> O <sub>3</sub> with 5% Fe addition, (c) 90% Al <sub>2</sub> O <sub>3</sub> with 10% Fe addition, (d) 95% Al <sub>2</sub> O <sub>3</sub> with 5% Cu addition, (e) 90% Al <sub>2</sub> O <sub>3</sub> with 10% Cu addition .....	30
Figure 4.7: Combined Data of Alumina-iron Composites .....	32
Figure 4.8: Combined Data of Alumina-copper Composites .....	33



## LIST OF TABLES

Table 3.1: Compositions of ceramic composites.....	17
Table 4.1: Concentrations and Densities of Powders.....	21
Table 4.2: Densities of Alumina-iron Ceramic Composites .....	22
Table 4.3: Densities of Alumina-copper Ceramic Composites .....	22
Table 4.4: Flexural Strength of Samples with Various Compositions .....	26

# CHAPTER 1 INTRODUCTION

## 1.1 Background of Study

Composites are multiphase engineered materials that artificially made to fulfil the market needs. There are three main groups of matrices which are metals, polymers and ceramics, and two major forms of reinforcements, namely fibres and particles. Various combinations of matrix and reinforcement such as aluminium-alumina, copper carbide, kenaf-polypropylene and etc. are fabricated in order to bring together the mechanical properties that neither material can achieve on its own. Powder metallurgy technique is a widely selected method to fabricate composites. This technique enables wide range control on materials composition and has high microstructure forming capability at the same time [1].

One of the main purposes of ceramic matrix composites (CMC) is to achieve high fracture toughness. For metal matrix composites and polymer matrix composites, they are usually targeted to enhance yield stress, tensile stress and creep resistance. According to Brent [2], there is an increasing demand of materials which is suitable for high temperature applications. Non-reinforced ceramics with high bond energies actually fulfilled this requirement, but its brittleness limited the application. With reinforced materials added to the ceramics, these reinforcements improve the toughness by resisting the initiation and propagation of cracks. When CMC is impacted, the reinforcements embedded in the ceramics absorb the energy and stop the growing cracks.

Alumina, a type of ceramics that refined from bauxite, can be considered as the most abundant material in ceramics aside from silicates. Due to its abundancy, the cost of alumina is relatively low compared to other ceramics materials. Comparing alumina to silica and zirconia, they have similar mechanical properties such as high hardness and brittle, but alumina has superior properties in terms of thermal conductivity and elastic modulus [3]. For the selection of metal powder reinforcements, both iron and copper are ductile which can improve alumina's brittleness and copper has relatively low melting points to enable liquid phase sintering during the sintering process.

## **1.2 Problem Statement**

Ceramics and metals have their own unique mechanical properties. For ceramics to achieve high flexural strength, the sintering temperature and energy needed is high; whereas for metals, the energy required is relatively low but metals could not achieve ceramics' high hardness. The goal of reinforcing ceramics with metals is to obtain a more desirable combination of properties. It has been proven in He et al.'s [1] study of alumina-iron composites and Travitzky's [4] study of alumina-copper composites that ceramic matrix with certain volume of metal additions exhibit superior mechanical properties in terms of fracture toughness and flexural strength compared to pure alumina. However, the mechanical properties of alumina composites do not increase or decrease proportionally with the volume of metal reinforcement. Therefore, this study is conducted to determine the optimum iron powder and copper powder content as additives to the alumina-iron and alumina-copper composites respectively to enhance the flexural strength.

## **1.3 Objective**

This project is focusing on characterization and properties of alumina-iron and alumina-copper ceramic composites. Powder metallurgy is selected as the fabrication method to prepare alumina matrix composites test specimens by using alumina powder, iron powder and copper powder.

The objectives of this project are:

1. To study the effects of iron and copper additions in density and flexural strength of the alumina matrix composites, respectively. The optimum iron and copper additions in the alumina composites will be determined.
2. To evaluate the microstructure-properties relationship for the alumina-iron and alumina-copper matrix composites.

## **1.4 Scope of Study**

The scope of this project is limited to the followings:

1. Experiment on the two different volume percentages (5% and 10%) of iron powder and copper powder content to the density and flexural strength of respective alumina matrix composites test specimens prepared based on MPIF standard 60.
2. Determine density and flexural strength of alumina-iron and alumina-copper composites based on MPIF standard 41.
3. Observe microstructures of alumina matrix composites by using Scanning Electron Microscope.

## CHAPTER 2 LITERATURE REVIEW

### 2.1 Ceramic-Metal Composites

Ceramic-metal composite is a structural material that consists of two or more combined constituents, with ceramic matrix reinforced by metallic reinforcing phase materials in the form of fibres, flakes or particles [5]. Ceramic acts as a continuous phase in composites, it covers the reinforce metals and provides shape of the structures [2]. Properties of ceramic-metal composites are depending on size, volume fractions of reinforcement and nature of matrix-reinforcement interface [6].

The additions of metals to ceramics have the ability to increase the density, fracture toughness and flexural strength of ceramics [7-9]. Past research about the microstructures and mechanical properties of pure alumina and alumina-iron composites proved that with iron additions to alumina, the composites able to achieve higher fracture toughness [1, 10]. The drawback of metal additions to ceramics is reduction in hardness due to ductility of metal [1, 11].

### 2.2 Rule of Mixtures

Rule of mixtures is an approach to predict the composite material properties such as Young's modulus, shear modulus, Poisson's ratio, tensile strength and density. According to the rule of mixtures, composites properties are estimated by the volume fractions of individual components [12].

For a composite, the total volume fraction of matrix and reinforcement is unity, as in (1).

$$V_m + V_r = 1 \quad (1)$$

Equation (2) can be applied to estimate the composite modulus in the case where loads are applied longitudinally to the reinforcement direction, also known as isostrain condition.

$$E_c = V_m E_m + V_r E_r \quad (2)$$

Other than modulus of elasticity, the strength of composite can be calculated by using equation as shown in (3).

$$\sigma_c = V_m\sigma_m + V_r\sigma_r \quad (3)$$

By applying the same rule, the theoretical density of composite can be estimated by the densities and volume fractions of both matrix and reinforcement as in (4).

$$\rho_c = V_m\rho_m + V_r\rho_r \quad (4)$$

## 2.2 Alumina Powder

Alumina, or Aluminium Oxide,  $\text{Al}_2\text{O}_3$  has been widely used in engineering applications due to its availability in abundance, relatively in good strength, wear and corrosion resistance, and reasonably priced. The typical applications of alumina are as grinding media, thread and wire guides, laboratory instrument tubes and etc.

Alumina is bonded by ionic interatomic bonding, with molecular weight of 101.96 g/mol. It has a high melting temperature of 2072°C. Alumina is graded based on its purity, alumina with high purity grade contains lower amount of impurities and thus the cost of production is higher. The purity levels of alumina are ranging from 85.0% to 99.9 % [13]. The characteristics and mechanical properties of alumina at room temperature based on the grades can be referred in Appendix A.

## 2.3 Iron Powder

Iron, Fe is one of the cheapest, most abundant and most useful metal. It is well known as an essential element for steel. Iron has a relative high melting temperature, 1538°C and pore-free density of iron is 7.87 g/cm<sup>3</sup> [14]. The mechanical properties of iron powder depend on its purity and the manufacturing method.

There are two main types of iron powder; sponge iron powder and water-atomized iron powder. According to Pease [14], the internal structure of sponge iron powder is spongy and the surface is highly irregular. This lowered its compressibility and results in high percentage of porosity. For water-atomized iron powder, they are pure, soft and highly compressible. The common applications of iron powder in powder

metallurgy are such as bearings and filter parts, wear resistance parts, machine parts and etc.

## 2.4 Copper Powder

Copper has a melting point of 1085°C and density of 8.94 g/cm<sup>3</sup>. Besides, it has high thermal conductivity, 385 W/mK which helps in rapid heat disperse. Copper powder is applicable in refractory materials, industrial and machine parts such as brake linings. Copper possess high ductility, which is 60 percentage elongation at room temperature and its low hardness make it a suitable reinforcement to improve the fracture toughness of ceramic composites [15].

## 2.5 Powder Metallurgy

Powder Metallurgy, P/M is considered as an economical manufacturing method to fabricate high-precision complex parts with high quantity. The applications of P/M are extensive; a wide variety of products such as structural parts, tribology parts, and magnetic parts can be fabricated by utilizing P/M technology. It is worth noting that “*P/M includes the processing of ceramic parts from powder, although the term refers to metal part*” [16]. P/M gives freedom to the composition and microstructures of the raw materials used; this enables the fabrication of various types of composites. P/M can be divided into 3 main processing steps; they are mixing and blending of powders, compaction, and sintering [17].

In the first processing step of P/M, different sizes of same chemical composition powders are blend together, whereas powders with different chemical compositions are mixed to achieve uniform distribution. This step can be done by utilizing rotating containers and stirring mechanism. Mixing time is ranging from minutes to days. Prolonged mixing time can cause reduction to the size of particles and alteration in particles shape [16].

Cho et al. [18] stated that it is a challenge for reinforced materials to distribute uniformly and well separated in the matrix. In their study focused on carbon nanotubes loaded CMCs, the high aspect ratio of carbon nanotubes formed agglomeration and

caused ceramics unable to fully penetrate through the carbon nanotubes. This hindered the reinforcements from contributing to the mechanical properties.

After uniform distribution of powder is achieved, comes to the compaction process. This process relies on external source to provide the part with sufficient green strength to undergo sintering process. Compaction can be done by pressing, casting, extruding and etc. The compacting pressure depends on the powder used; the compacting pressure for iron, copper and alumina is 350-800MPa, 207-248MPa and 110-140 MPa respectively [19]. The material and powder characteristics do affect the compressibility and green density. German [17] stated that small, hard and sponge powders are difficult to compact, they may show high compressibility at first but spring back during ejection.

Based on German [17], “*sintering is the bonding together of particles by diffusion at high temperature.*” Sintering time depends on various factors such as particles diameter, density of green compact and sintering temperature. Two common types of sintering in powder metallurgy are solid state sintering and liquid phase sintering.

For solid state sintering process of heterogeneous material, the sintering temperature is below the melting points of both components. Diffusion between particles occurs in solid state in order to achieve reduction of porosity [20]. If liquid phase sintering takes place in heterogeneous mixture, the sintering temperature which is higher than one of the components’ melting point causes the particles to melt and thus fill in the pores between the particles. According to Biswas [21], his study concluded that liquid phase sintering has advantages for SiC production. SiC sintered by liquid phase able to achieve tailored microstructures, higher fracture toughness with lower sintering temperature compared to solid state sintering. Other than this, in Hernandez’s study of alumina-copper composites, with liquid phase sintering, copper additions melted wet the alumina and thus reduced the porosity [11].

## **2.6 Microstructures of Composites**

It is worth noting that increasing loading fractions of reinforcement will not necessarily further enhance the composites. High loading fractions of reinforcement particles can



cause agglomeration, shortage of matrix to 'cover' the surface of all the reinforcement particles [18].

This is supported by Rahimian et al.'s [22] research on effect of reinforcement particles volume and size to the microstructure of Al-Al<sub>2</sub>O<sub>3</sub> composite. The research concluded that, using the same volume of alumina as reinforcement, sample with 3µm particle size has lower homogeneity compared to samples with particle sizes of 12µm and 48µm due to high inter-particle friction and agglomeration.

From the same study [22], by setting the alumina particles size as constant, increasing the volume of alumina results in finer grain sizes and lower distribution homogeneity. This is contradicted with Vazquez's study of titanium additions to alumina, his results showed that increasing titanium content aided in grain growth [23]. The contradiction of results is due to the narrow range of reinforcement weight percentage, 0.5 to 3.0wt % as discussed by Vazquez, further increment of titanium content may cause adverse effect to grain growth.

## **2.7 Green, Sintered and Relative Densities of Composites**

Green density is the density of an unsintered P/M part and can be measured after compaction whereas sintered density is the density measured after sintering process is done [17]. Both green and sintered densities can be measured and compared to its theoretical density calculated from using rule of mixture. For relative density, it is the ratio of density measured to the theoretical density calculated by rule of mixture. Relative density is usually present in percentage.

The densities of composites can be affected by various factors such as sintering temperature, volume fractions and type of reinforcement used. In Tani's [24] study, he investigated the influence of pressureless-sintering temperature on the relative density of SiC – 20 vol.% TiB<sub>2</sub>. The research concluded that increasing of sintering temperature did improve the relative density and reduce the open porosity. Rahimian et al. [25] also stated that by increasing sintering temperature, the diffusion rate is higher and thus the relative density increases.

With increasing volume of metal reinforcements such as iron and copper to alumina ceramics, the sintered densities of composites increase [1, 11, 26]. This is expected because the densities of metals are higher than alumina. However, the relative densities of composites only increase up to an optimum volume of reinforcement, further additions of reinforcement particles resulted in adverse effect [1, 22].

## **2.8 Mechanical Properties of Composites**

From the past research, the mechanical properties commonly tested for alumina based composites are hardness and flexural strength. Various researchers reported that the hardness and flexural strength of alumina base ceramic composites are usually affected by parameters such as volume of metal reinforcement added and sintering conditions [1, 4, 7, 11, 26, 27, 28].

According to Hernandez et al. and Winzer et al. [11, 26], the increasing of copper content resulted in decrement of composite hardness. This is because of the ductility of copper. This is supported by He et al's study of iron addition to alumina [1]. In addition, similar results were reported by Ahamd et al. [28] in his study of carbon nanotubes additions to alumina. Low volume of carbon nanotubes did increase the composite hardness until an optimum level, but it decreased with further increment of reinforcement volume.

Other than hardness, the volume of metal reinforcement added also affect the flexural strength of ceramic composite. The study of carbon nanotubes additions to alumina increased the flexural strength of composite until 20% volume, the flexural strength decreased after that optimum level [28]. However, the flexural strength of carbon nanotubes reinforced alumina is still higher than pure alumina.

For sintering conditions, in Travitzky's [4] study of pressure-assisted and pressure-less infiltrated  $\text{Al}_2\text{O}_3$ -Cu composites, he concluded that pressure assisted infiltrated  $\text{Al}_2\text{O}_3$ -Cu exhibit highest bonding strength and Vickers hardness followed by pressure-less infiltrated  $\text{Al}_2\text{O}_3$ -Cu, then pure alumina.

### 2.8.1 Flexural Test

Flexural test can be considered as a substitute of tensile test for ceramics, it is a more suitable test because of ceramics' brittleness and low elasticity. By performing flexural test, mechanical properties of ceramics such as fracture strength, flexural strain and flexural modulus can be determined. There are two types of flexural test, which are three-point and four-point bending test. In these bending tests, the top surface of specimen is subjected to compression state whereas the bottom surface is in tension [3]. Equation (5) can be used to compute the flexural strength for specimen with rectangular cross section.

$$\sigma_{fs} = \frac{3F_f L}{2bd^2} \quad (5)$$

By performing bending test, fracture toughness, a measure of “*ceramic material's ability to resist brittle fracture when a crack is present*” [3] can also be determined. Fracture toughness can be expressed in equation as shown in (6).

$$K_{Ic} = Y\sigma\sqrt{\pi a} \quad (6)$$

## CHAPTER 3 METHODOLOGY

### 3.1 Research Methodology

The research flow of the project is shown in Figure 3.1.

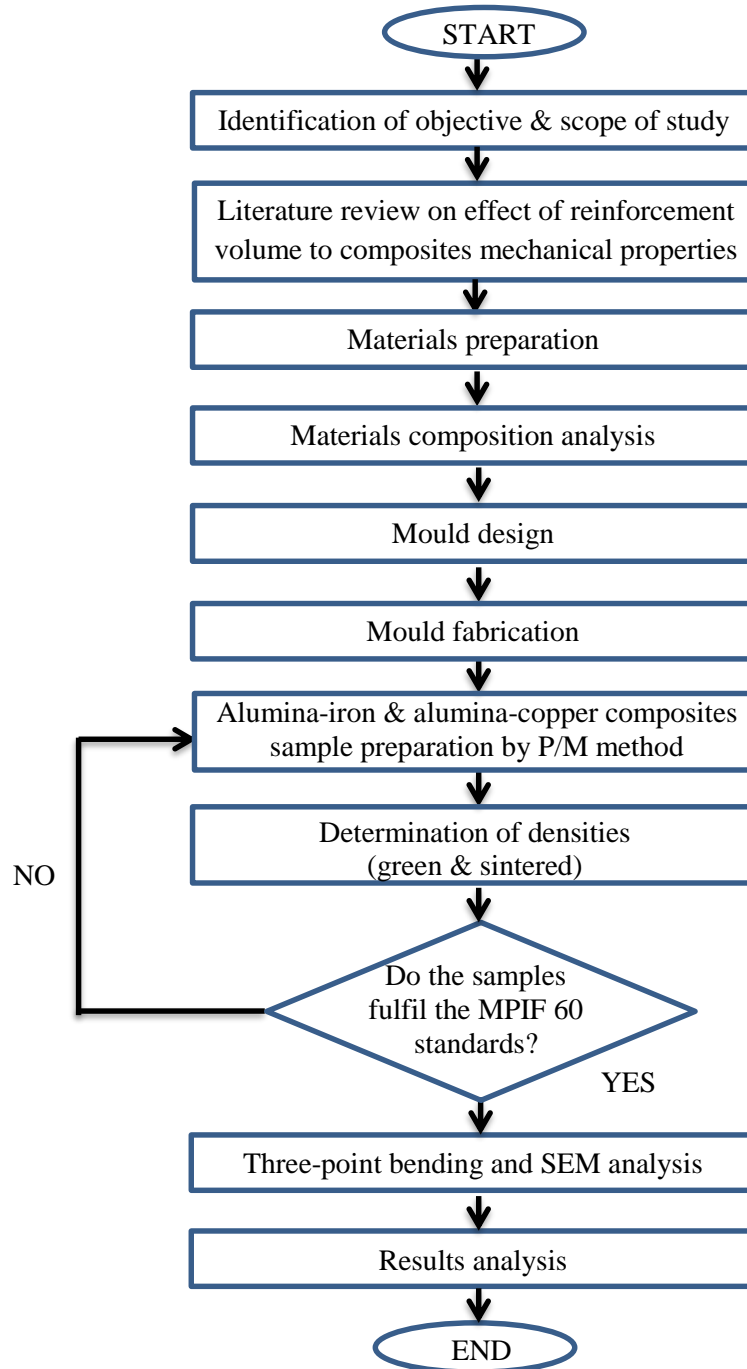


Figure 3.1: Project Flow Chart

Throughout FYP1 and FYP2, the project activities will be carried out based on the research flow as shown in Figure 3.1. The project activities involved are mainly experimental works. Throughout FYP1, the project activities are completed up to mould fabrication. After that, samples are fabricated using the mould prepared. The samples are then undergone three-point bending test and microstructural analysis. The results obtained are tabulated and discussed in Chapter 4.

### 3.2 Project Gantt Chart

The project Gantt charts for FYP1 and FYP2 are shown in Figures 3.2 and 3.3 respectively. The project activities planned to be completed throughout these two semesters are listed. Besides, key milestones are also indicated in the Gantt charts.

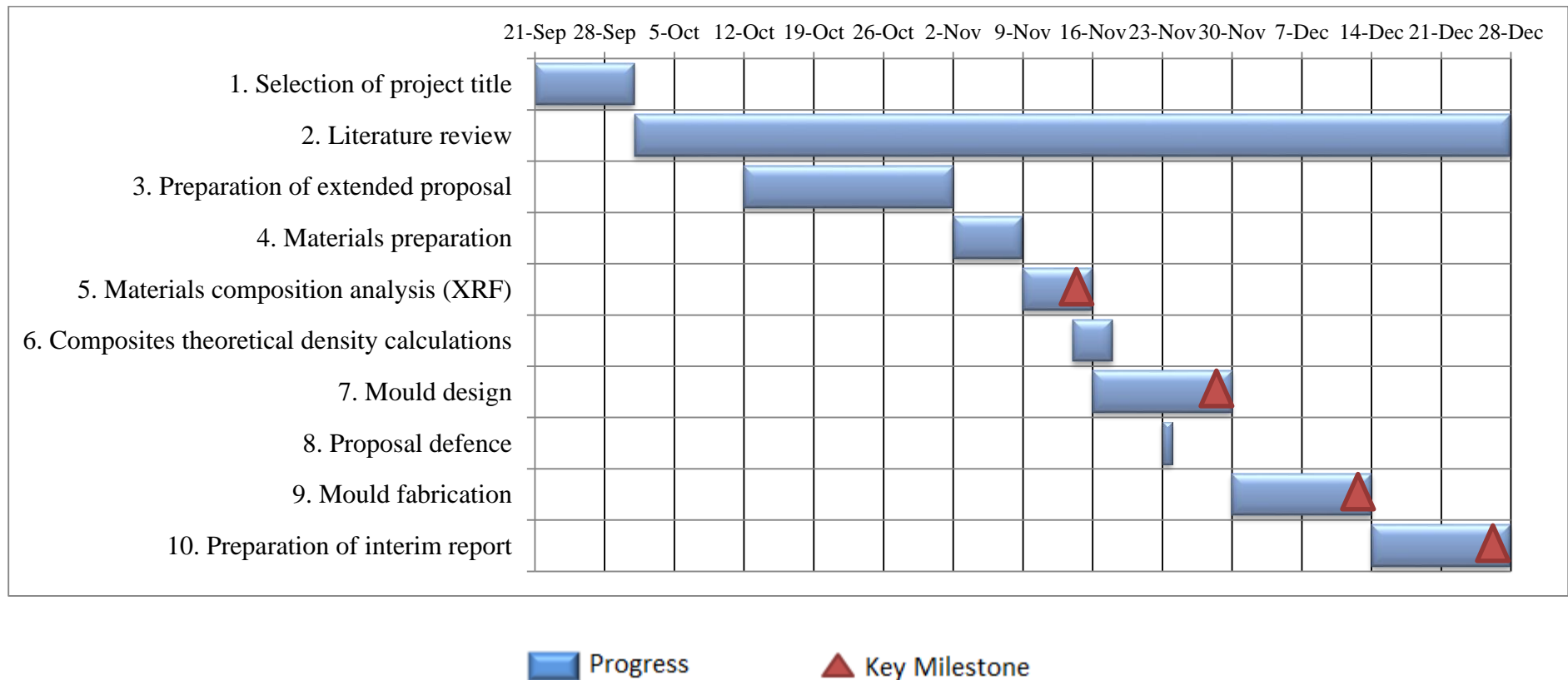
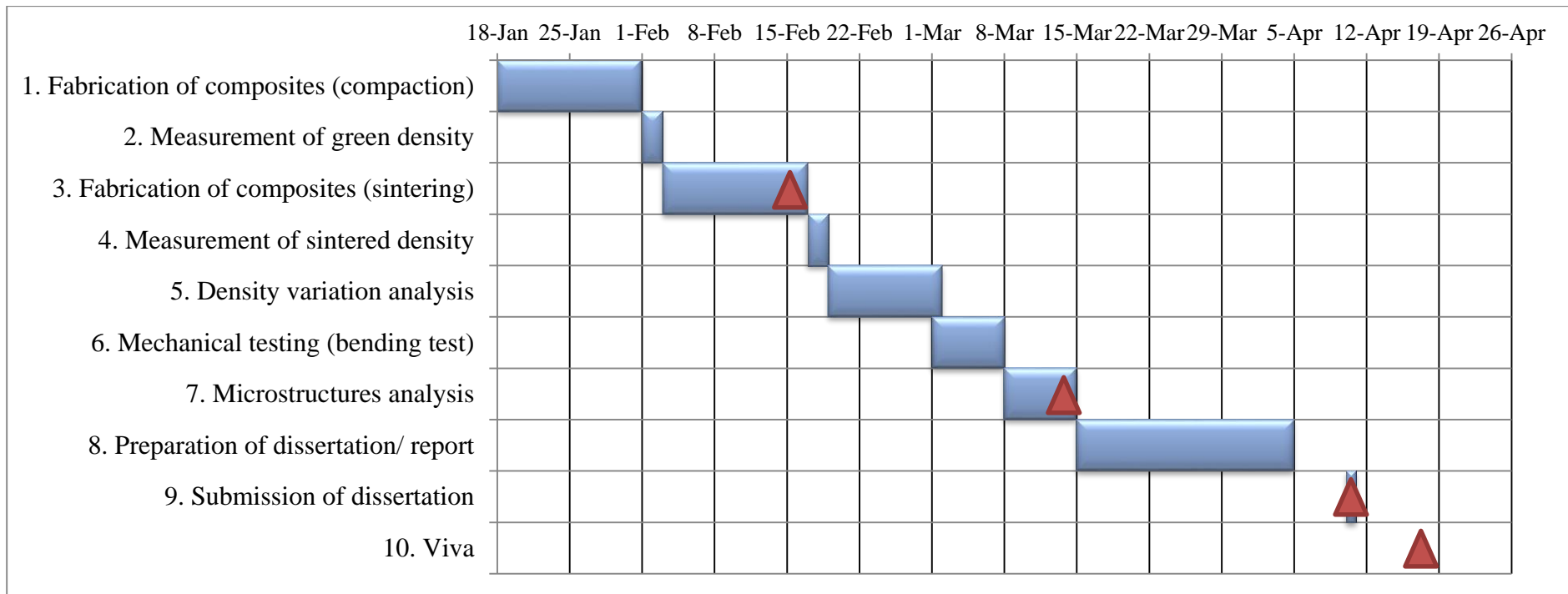


Figure 3.2: Project Gantt Chart (FYP 1)



■ Progress      ▲ Key Milestone

Figure 3.3: Project Gantt Chart (FYP 2)

### 3.3 Key Milestones

Figure 3.4 presents the key milestones of this project. There are eight key milestones to be achieved in order to meet the objectives of this project.

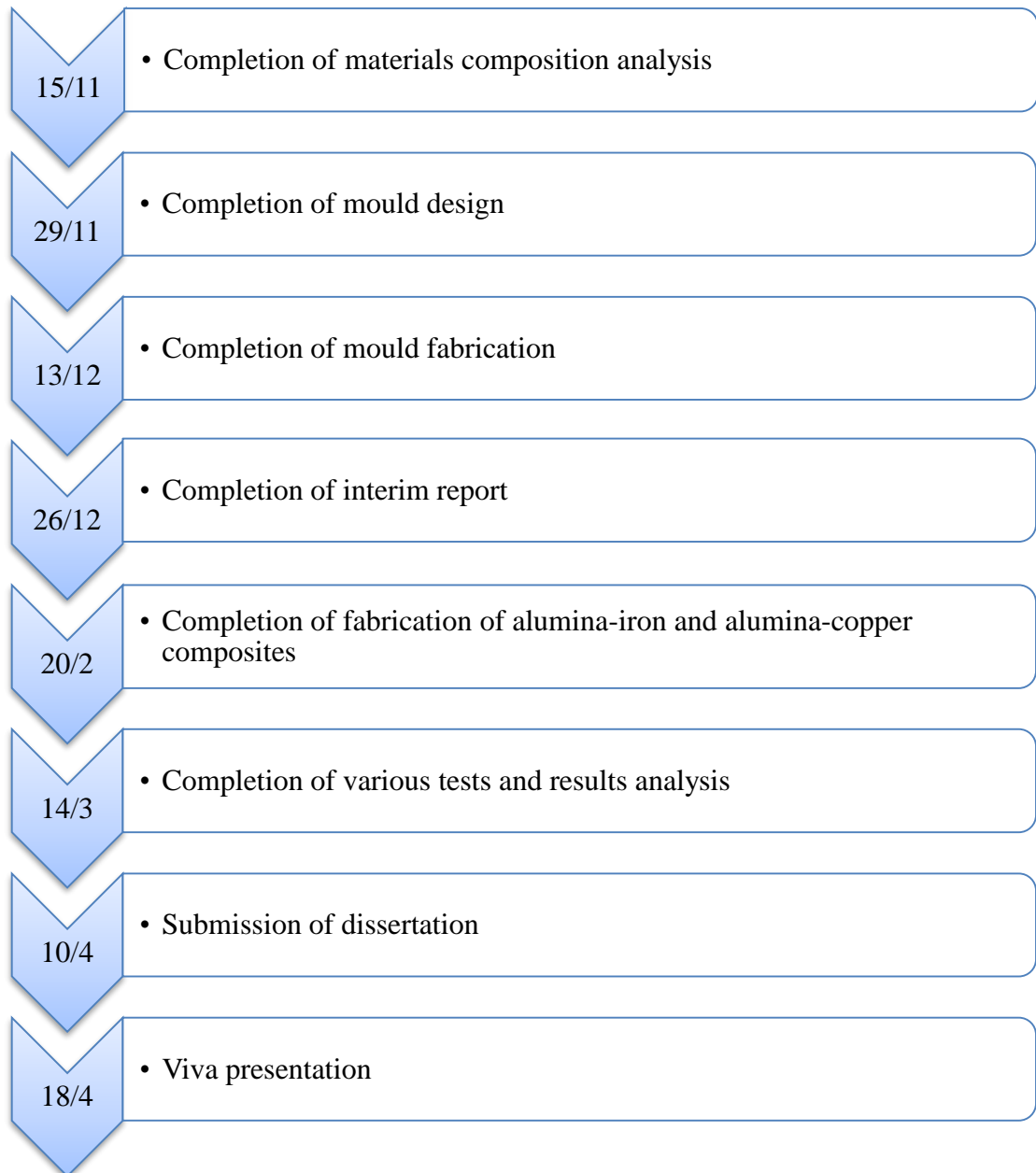


Figure 3.4: Project Key Milestones



### **3.4 Experimental Works**

The three main processes to prepare alumina-iron and alumina-copper ceramic composites test specimens are mixing process, compaction process and sintering process.

#### **3.4.1 Raw Materials and Equipment**

The materials used for preparing alumina-iron and alumina-copper composites are alumina powder, iron powder and copper powder. The size of the alumina and copper powders are 63 $\mu$ m, and iron powder with size of 10 $\mu$ m. The binder needed for these composites is paraffin wax.

The equipment and machines needed for ceramic composites fabrication and results analysis are:

- Mettler Toledo digital weighing scale
- XRF spectrometer
- Tubular mixer
- Compression machine
- Sintering furnace
- Universal testing machine
- Scanning electron microscope

The photo of all the equipment needed are attached in Appendix B.

#### **3.4.2 XRF analysis**

The alumina, iron and copper powders are acquired from laboratory. XRF analysis had been carried out to determine the composition of the powders. This is to determine the purity of the powders which will affect the density. 7g of each powder are needed to perform XRF analysis.

### 3.4.3 Mixing Process

The amount of powders required are weighed using the Mettler Toledo digital weighing scale. Amount of powders needed for all samples are calculated from the volume percentages listed in Table 3.1. The sample calculation for conversion of volume percentage to mass is shown in Appendix C. Five samples are needed for each composition. A total of 25 samples with 5 different compositions have to be prepared. The total amount of alumina, iron, copper and paraffin wax needed to prepare all the samples is 225g, 15g, 17g and 7.7g respectively.

The alumina and iron powders are mixed with 3 wt% of paraffin wax using tubular mixer for 30 minutes, same for alumina and copper powders. Paraffin wax is added to aid in binding of powders during the compaction process. After mixing process is completed, the mixed powders are measured to a weight of 9.0g to 12.0g, depending on the composition of the mixtures.

Table 3.1: Compositions of ceramic composites

Composites	Volume percentage, % vol			Mass, g		
	Alumina, Al <sub>2</sub> O <sub>3</sub>	Iron, Fe	Copper, Cu	Alumina, Al <sub>2</sub> O <sub>3</sub>	Iron, Fe	Copper, Cu
<b>Pure alumina</b>	100	-	-	9.6	-	-
<b>Alumina-iron composites</b>	95	5	-	9.1	1.0	-
	90	10	-	8.6	2.0	-
<b>Alumina-copper composites</b>	95	-	5	9.1	-	1.1
	90	-	10	8.6	-	2.3

### 3.4.4 Compaction Process

Next, the mixed powders are placed into a through-hole mould with a rectangular-shaped cavity. The mould design is attached in Appendix D. The mixed powders are compacted using compression machine under 375MPa. With this pressure, the compaction force transferred to the mixed powders is 200kN. The force can be calculated by using (8).

$$Force = Pressure \times Area \quad (8)$$

### 3.4.5 Sintering Process

In this process, compacts prepared are sintered in a sintering furnace with Nitrogen atmosphere. The samples are sintered at a heating rate of 5°C/min and when the temperature reached 730°C, dwell for 15 minutes. After that, continue sintering until 1100°C then dwell for 45 minutes. After the sintering process is done, the samples will be cooled to room temperature naturally. The sintering cycle is showed in Figure 3.5.

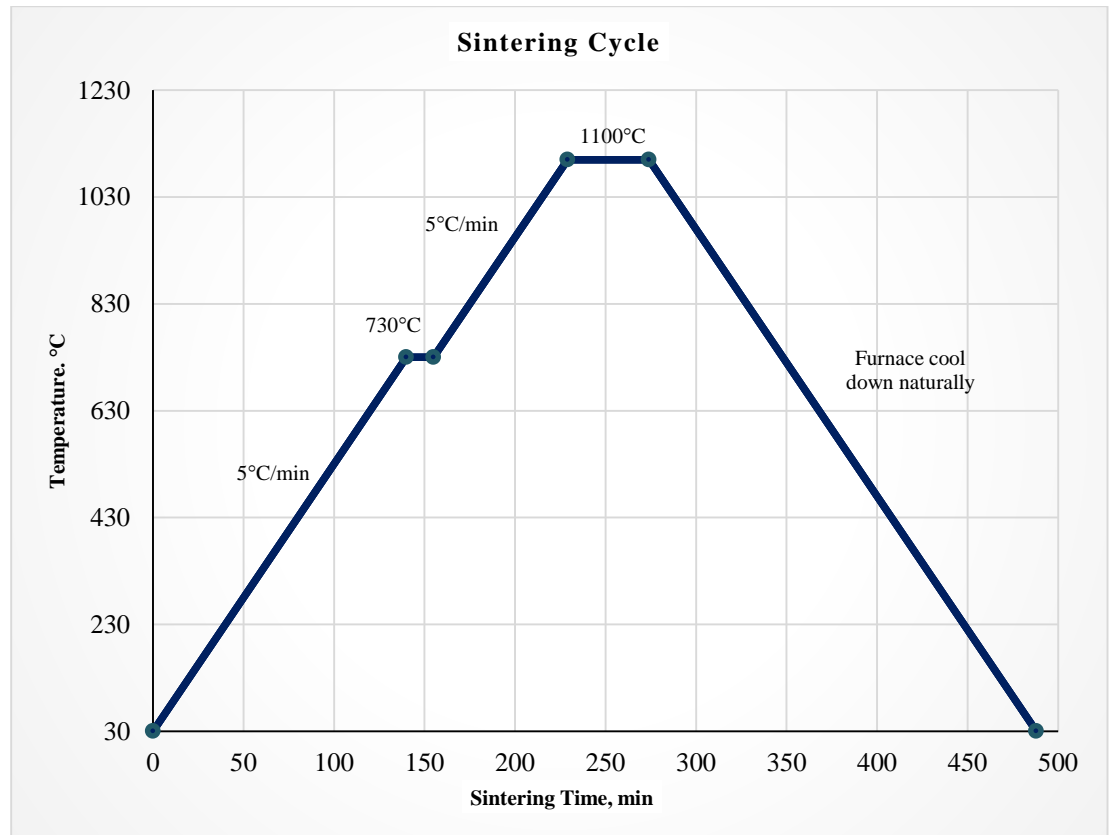


Figure 3.5: Sintering Cycle

### **3.4.6 Measurement of Green and Sintered Densities**

The green and sintered densities of samples are measured and recorded. The green densities are measured after the completion of compaction process whereas sintered densities are measured after the sintering process. The sintered densities measured are thus compared with the theoretical densities calculated based on the rule of mixtures. Besides, the relative densities in term of percentage are calculated.

## **3.5 Samples Analysis**

Analysis of samples are carried out after the completion of experimental works. The analysis included in this project are characterization of samples' microstructures and flexural strength of the samples.

### **3.5.1 Three-Point Bending Test**

Three-point bending test is performed based on MPIF standard 41. Universal testing machine is used for this bending test. The sample is clamped to the machine with a span of 25.4mm and increasing load is applied to the center of sample at a speed of 0.50mm/min until it breaks. The flexural strength is thus determined from data recorded.

### **3.5.2 Microstructure**

The scanning electron microscope is used to observe the microstructures of the samples prepared. A magnification of 1000x is used and the micrographs obtained are analysed.

## CHAPTER 4 RESULTS AND DISCUSSION

### 4.1 Powders Shape, Concentration and Density

From SEM analysis of alumina, iron and copper powder, the shape and size of powders are determined before the mixing process is performed. Figure 4.1 demonstrates the micrographs of alumina, iron, copper powder and paraffin wax respectively under 500x magnification.

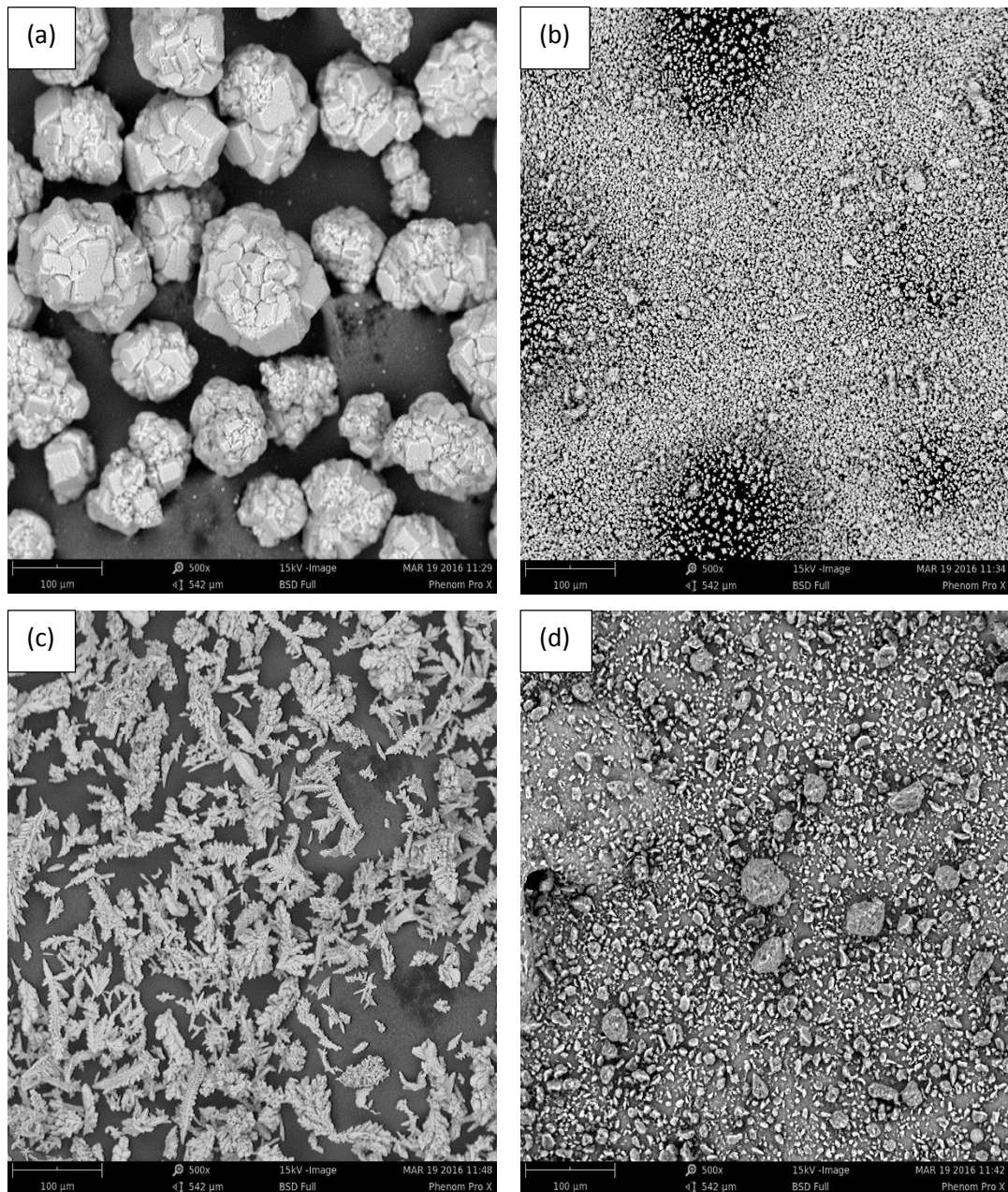


Figure 4.1: SEM micrographs of (a) Alumina powder, (b) Iron powder, (c) Copper powder, (d) Paraffin wax

From Figure 4.1(a), alumina powder is blocky in shape compared to other type of powder. It has a size of 63 $\mu\text{m}$ . For iron powder, the SEM micrograph is presented in Figure 4.1(b). Iron powder is spherical in shape and 10 $\mu\text{m}$  in size. From Figure 4.1(c), it can be observed that copper powder is in flake shape and has a size of 63 $\mu\text{m}$ . For the binder, paraffin wax is used and its micrograph is showed in Figure 4.1(d). Paraffin wax has an irregular shape and size.

From the XRF analysis, the concentrations of the alumina, iron and copper powders are determined. For alumina powder, its density varies with the concentration. The densities of alumina powders with different concentrations are attached in Appendix A. The powders concentrations and densities are listed in Table 4.1.

Table 4.1: Concentrations and Densities of Powders

<b>Raw Material</b>	<b>Concentration, %</b>	<b>Density, g/cm<sup>3</sup></b>
<b>Alumina powder</b>	95.6*	3.75
<b>Iron powder</b>	99.5*	7.87
<b>Copper powder</b>	99.3*	8.94

\* The actual compositions are attached in Appendix E.

## 4.2 Composites Density

The theoretical densities of composites with various compositions are calculated by using rule of mixture from the powder density obtained through XRF analysis. Under the compaction pressure of 375MPa, alumina and copper are able to achieve their respective density as determined from XRF analysis. However, it is different case for iron. The suggested compaction pressure for iron is ranging from 350 to 800MPa, so the iron can only reach 6.6g/cm<sup>3</sup> under 375MPa. The iron density-pressure curve is included in Appendix F. This is considered in calculating the predict specimen density of alumina-iron composites. The mass and volume of samples are determined before and after sintering process. These data are used to compute the green and sintered densities.

The densities of alumina-iron and alumina-copper ceramic composites with various compositions are presented in Tables 4.2 and 4.3 respectively.

Table 4.2: Densities of Alumina-iron Ceramic Composites

Volume percentage, % vol		Density, g/cm <sup>3</sup>				
Alumina	Iron	Theoretical	Predict (375MPa)	Green	Sintered	Relative,%
100	0	3.75	3.75	2.56	2.96	78.93
95	5	3.96	3.89	2.72	3.22	82.77
90	10	4.16	4.04	2.78	3.27	80.94

Table 4.3: Densities of Alumina-copper Ceramic Composites

Volume percentage, % vol		Density, g/cm <sup>3</sup>				
Alumina	Copper	Theoretical	Predict (375MPa)	Green	Sintered	Relative,%
100	0	3.75	3.75	2.56	2.96	78.93
95	5	4.01	4.01	2.69	3.11	77.56
90	10	4.27	4.27	2.87	3.43	80.33

Below are the sample calculations of theoretical, predict and relative density in percentage for alumina-iron ceramic composites with 95% alumina and 5% iron. For the green and sintered densities, the values are the average of 5 samples prepared. The figures of sintered samples with various compositions are included in Appendix G. For the mass, volume and density of each sample, they are tabulated and attached in Appendix H.

$$\begin{aligned}
 \text{Theoretical density, } \rho_{th} &= V_m \rho_m + V_r \rho_r \\
 &= 0.95(3.75) + 0.05(7.87) \\
 &= 3.96 \text{g/cm}^3
 \end{aligned}$$

$$\begin{aligned}
 \text{Predict specimen density, } \rho_{specimen} &= V_m \rho_m + V_r \rho_r \\
 &= 0.95(3.75) + 0.05(6.60) \\
 &= 3.89 \text{g/cm}^3
 \end{aligned}$$

$$\begin{aligned}
 \text{Relative density, } \rho_r &= \frac{\text{sintered density}}{\text{predict density}} \\
 &= \frac{3.22}{3.89} \\
 &= 82.77\%
 \end{aligned}$$

Figures 4.2 and 4.3 show the graph of density against volume percentage of iron and copper in alumina-iron and alumina-copper composites respectively. Based on Figures 4.2 and 4.3, the theoretical and predict densities are higher compared to the sintered densities of samples produced. It can be observed that the sintered samples have significant increment in densities compared to their respective green densities. This indicated that the porosities of samples are reduced by sintering process. The trend of theoretical, predict, green and sintered densities of alumina-iron and alumina-copper composites increases as the volume percentage of iron and copper increases.

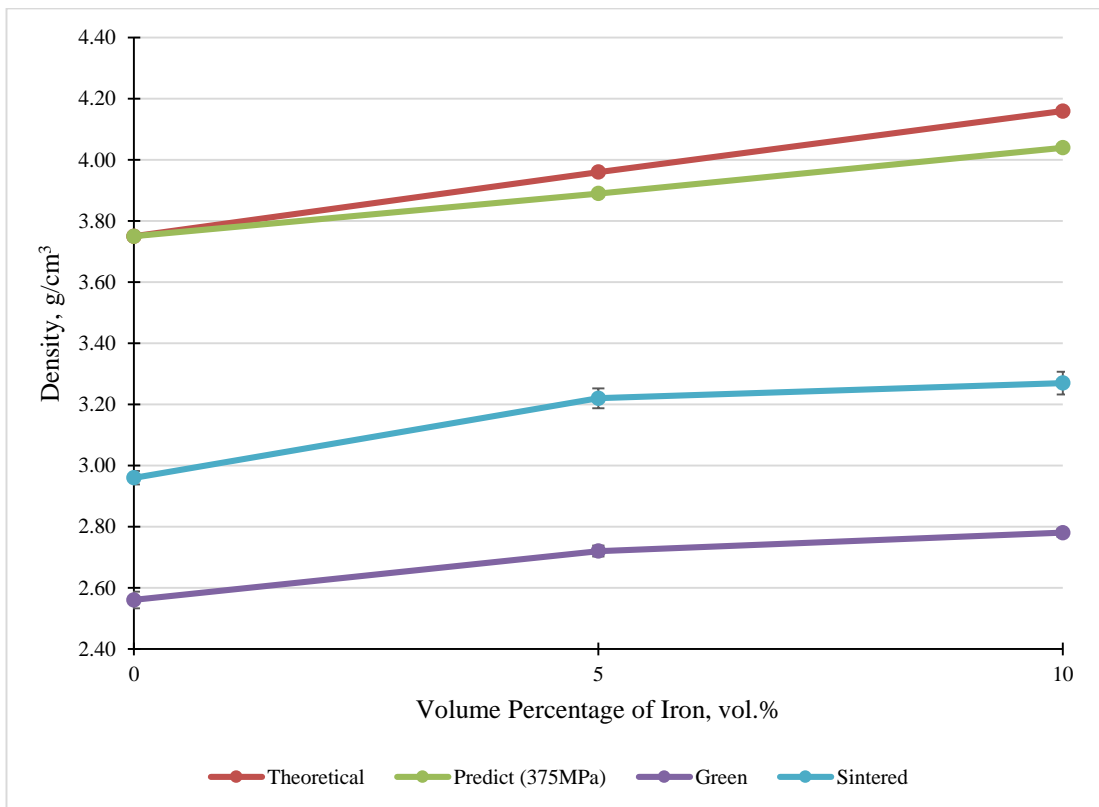


Figure 4.2: Graph of Density against Volume Percentage of Iron



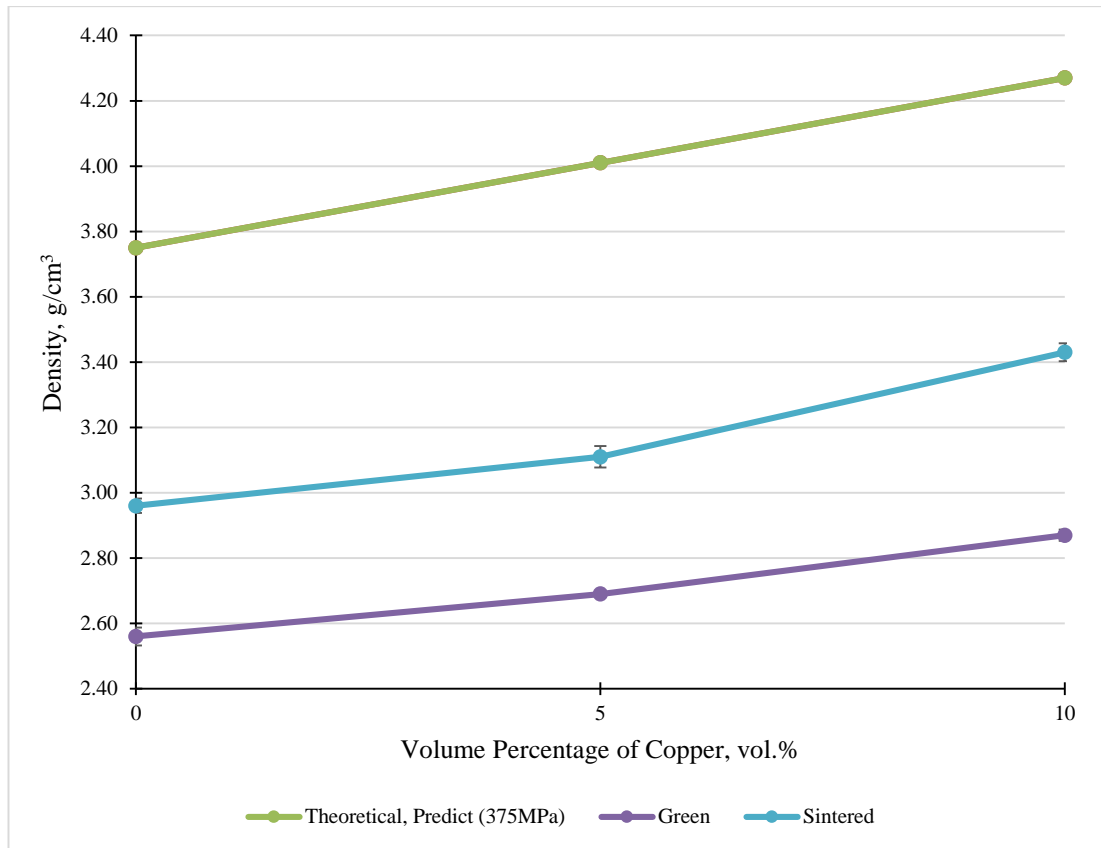


Figure 4.3: Graph of Density against Volume Percentage of Copper

With a sintering temperature of 1100°C, the alumina-iron undergone solid phase sintering, the atoms are bonded together in solid state under high temperature. For alumina-copper composites, the copper content is melted under 1100°C. This explained both alumina composites have higher sintered densities compared to green densities. However, the samples' sintered densities are unable to achieve respective predicted densities. This could be due to compaction process by using compression machine which is only able to perform uniaxial powder press under room temperature. Consequently, the sample produced will not achieve its predict density due to the lacking properties of green compacts. Based on relevant research [7, 24, 27], hot isostatic pressing is the method used to produce green compacts. The samples are place in a closed pressure vessel, high temperature and high gas pressure from all directions will be applied to produce green compacts. Comparing uniaxial pressing and hot isostatic pressing, the latter is able to produce green compacts with fully isotropic material properties. The relative density in percentage for both alumina-iron and alumina-copper are shown in Figure 4.4 below. The sintered density only achieved about 78% to 83% of their respective predict density.

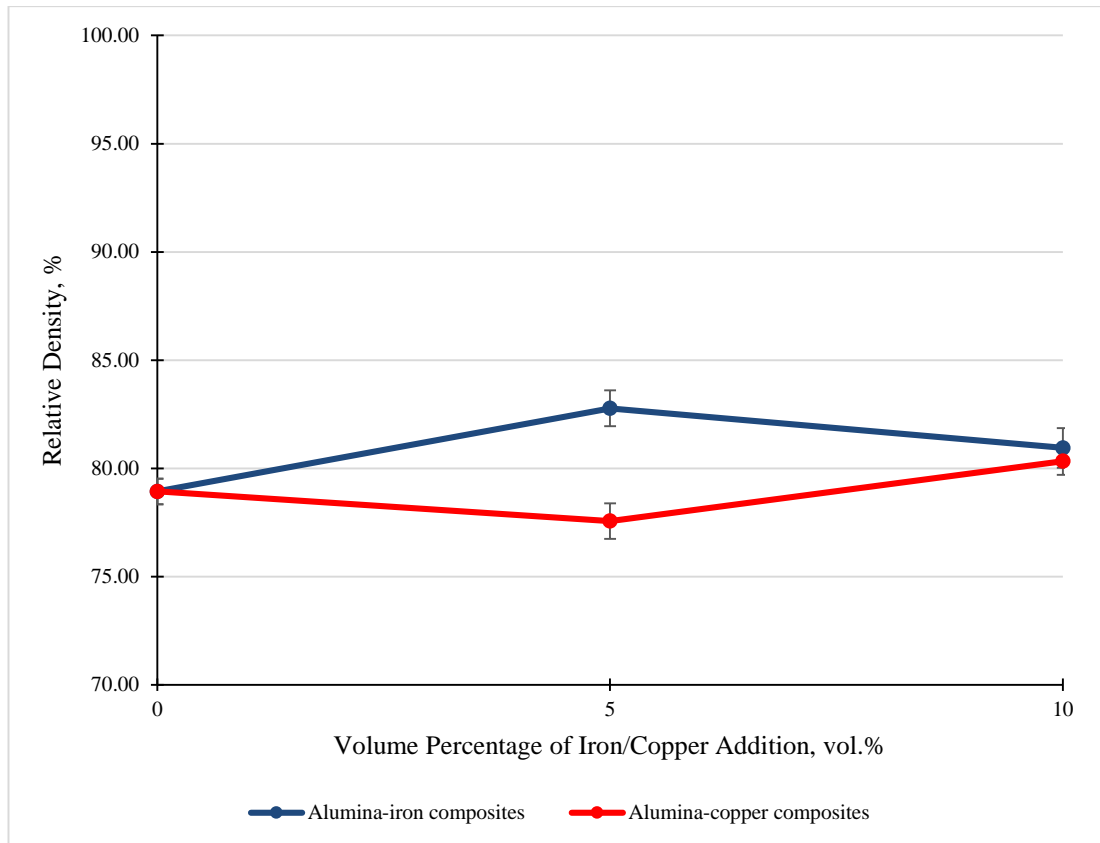


Figure 4.4: Graph of Relative Density against Volume Percentage of Iron or Copper

From Figure 4.2, the theoretical density increases linearly with the increment of iron percentage in samples. It can be observed that the trend of sintered density is slightly different from theoretical density, the increment in density reduced when the iron content is between 5% and 10%. This showed the iron content is reaching its optimum volume in alumina-iron composites. Based on He et al.'s [1] study, the density of alumina-iron functionally graded material undergone significant drop for iron content ranging from 30% to 70%. This proved that further addition of iron will not increase the alumina-iron density as predicted using rule of mixture. This could be caused by agglomeration of iron powder in the composites. There is a higher possibility of agglomeration with higher iron content. The formation of iron agglomerates prevents iron from incorporating their mechanical properties in alumina-iron composites.

From Figure 4.3, the trend of theoretical density of alumina-copper is linear, which is similar to alumina-iron. For sintered density, it increases with the addition of copper up to 10 vol.%. The sintered density has an obvious increment with the copper addition in the range of 5 vol.% to 10 vol.%. According to Hernandez et al. [11], the density of alumina-copper still increases significantly with addition of copper content as much as

30 vol.%. This can be explained by the lower melting temperature of copper compared to iron, copper melted during sintering process and liquefied copper able to wet and fill in the porosities of alumina-copper composites. This results in the increment of sintered densities with the volume percentage of copper.

### 4.3 Flexural Strength of Composites

Three-point bending test is performed using universal testing machine based on MPIF standards 41. For each composition of alumina-iron and alumina-copper composites, four samples were tested and the averaged flexural strength are tabulated in Table 4.4.

The flexural strength of pure alumina act as a constant to both type of alumina composites. However, the values of bending strength recorded in this work is relatively low. The bending strength of dense alumina with a size of 1 $\mu$ m able to achieved 280MPa whereas alumina with size of 4 $\mu$ m 320MPa to 420MPa [8, 15]. The low values of flexural strength can be caused by the larger size of alumina powder used, which is 63 $\mu$ m and relatively low sintered density of samples compared to respective predict density. The porosities in samples prepared lowering the flexural strength recorded.

Table 4.4: Flexural Strength of Samples with Various Compositions

Sample	Flexural strength, MPa
100% Al <sub>2</sub> O <sub>3</sub>	154.6
95% Al <sub>2</sub> O <sub>3</sub> – 5% Fe	284.6
90% Al <sub>2</sub> O <sub>3</sub> – 10% Fe	317.5
95% Al <sub>2</sub> O <sub>3</sub> – 5% Cu	120.2
90% Al <sub>2</sub> O <sub>3</sub> – 10% Cu	170.1

From Table 4.4, it can be observed that there is a remarkable enhancement on flexural strength of alumina-iron composites compared to pure alumina. With just a 5 vol.% of iron additions to the alumina composites, it nearly doubled up the flexural strength. Increasing the iron content to 10 vol.% further increased its flexural strength to 317.5MPa. However, the addition of 5 vol.% of copper to the alumina composites resulted a lower flexural strength compared to pure alumina. In contradict, the flexural

strength of alumina-copper composites increased after an increment of copper content up to 10 vol.%. To further analyse the data, a graph of flexural strength against alumina composites are plotted as shown in Figure 4.5.

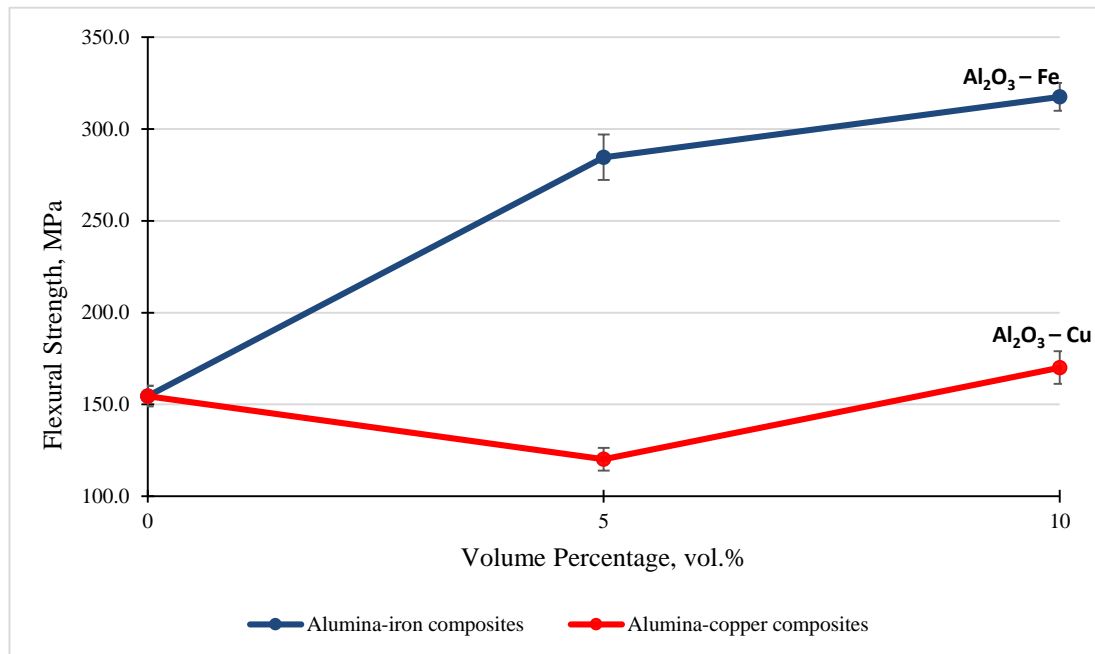


Figure 4.5: Graph of Flexural Strength against Volume Percentage of Metals

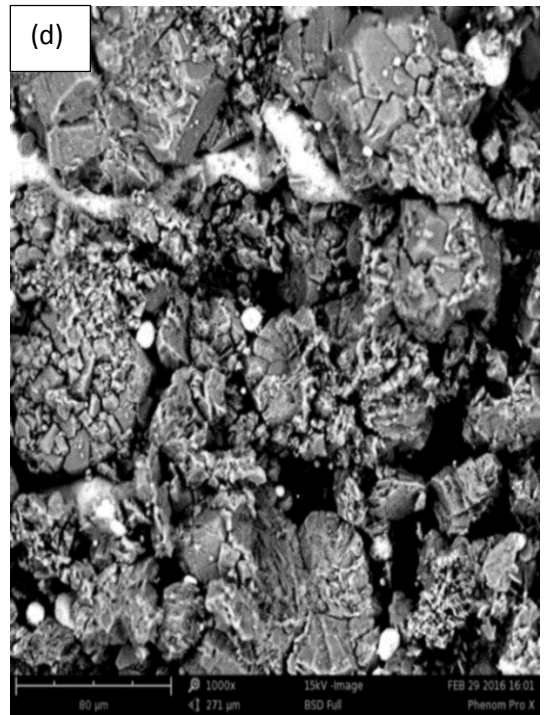
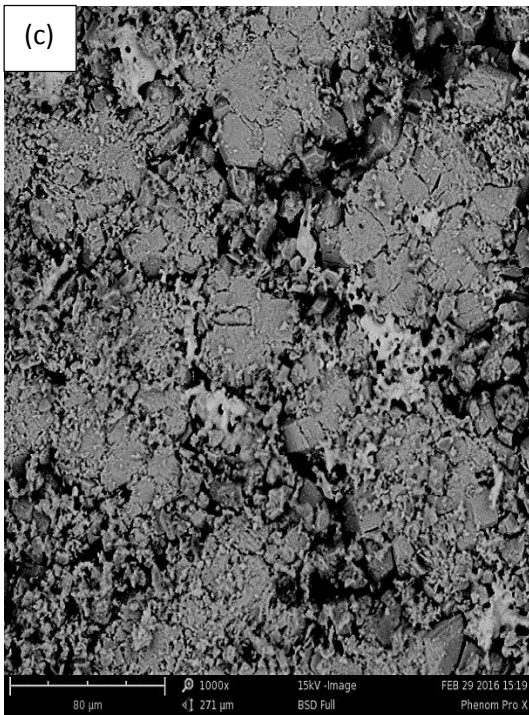
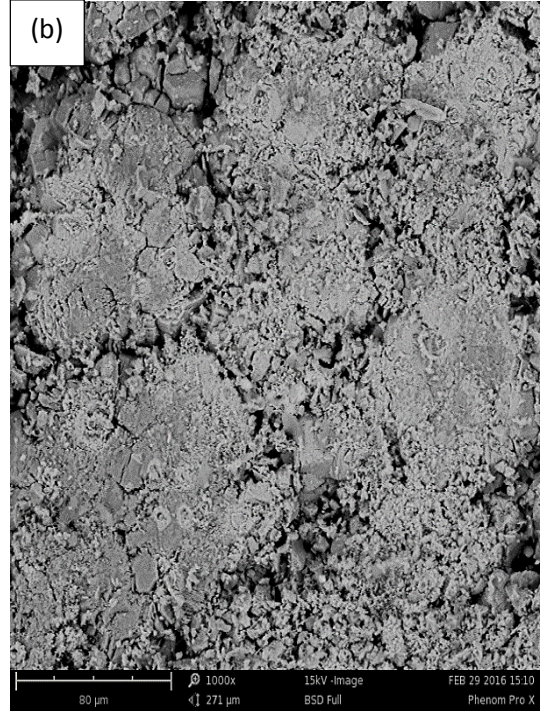
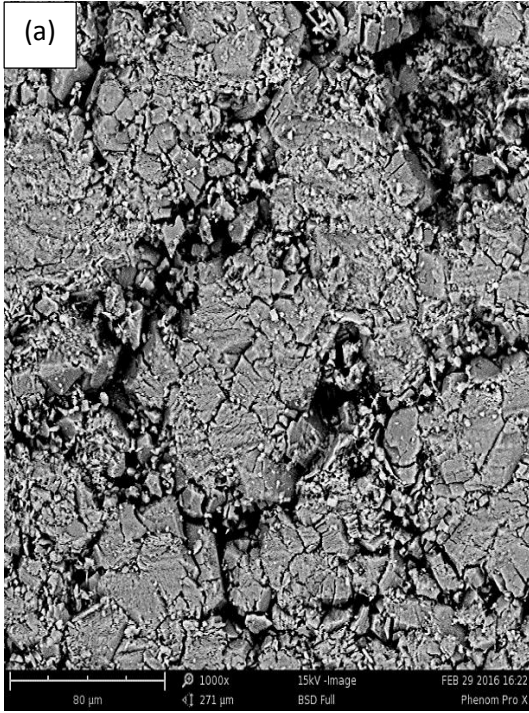
Based on Figure 4.5, the flexural strength of alumina-iron is generally higher than pure alumina. This finding is consistent with other works focusing on the variation of flexural strength of alumina-metal composites such as alumina-nickel, alumina-titanium, alumina-cobalt and alumina-molybdenum [4, 7, 8]. However, it is contradicting with He et al.'s study on alumina-iron functionally graded material consists of 30% to 70% iron addition to alumina. He et al. reported that the major cause of lower flexural strength of alumina-iron compared to pure alumina is the weak interfaces between layers of different composition within the functionally graded material [1]. The interface problem mentioned above had been overcome in this study by preparing samples of different composition individually. With this, the incorporation of iron to alumina successfully improved the flexural strength. Focusing on the alumina-iron composites with 5% to 10% iron addition, the flexural strength of composites is still increasing but with a lower rate. There is a possibility of agglomeration of iron increases above 5 vol.% iron content. The agglomerates of iron acts as a flaw that reduces the flexural strength moderately. The microstructures of the alumina-iron composites will be discussed in following section.

For alumina-copper composites, the trend recorded is different with alumina-iron. With 5 vol.% of copper, the flexural strength reduced to 120.2MPa, which is lower than the pure alumina. On the other hand, further increase of copper content to alumina composites did increased the flexural strength. Although the flexural strength of alumina with 10 vol.% of copper is higher than pure alumina, it is still lower than the value recorded by Travitzky [4]. According to Travitzky, the flexural strength of pressure-assisted infiltrated alumina-copper composites with 15 vol.% of copper is 355MPa [4], this is much higher than flexural strength of 10 vol.% copper obtained in this test. This justified that more copper should be added to alumina in order to fill in the pores and thus strengthen the alumina-copper composites.

Focusing on the low flexural strength of 5 vol.% copper alumina-copper composites, this can be caused by poor wettability of copper to alumina at 1100°C in nitrogen atmosphere. With this sintering temperature, the copper should be fully melted and soak into the interfaces of alumina. But with poor wettability, the pores could not be fully filled by the liquid copper in sintering process. This led to a lower flexural strength compared to alumina-iron composites which undergone solid phase sintering under the same condition. The microstructure of alumina-copper composites will be discussed in the following section to further analyse the cause of relatively low flexural strength recorded.

#### **4.4 Microstructures of Composites**

Microstructural analysis by scanning electron microscope, SEM with a magnification of 1000x is performed and the SEM micrographs of pure alumina and alumina-composites with various composition are shown in Figure 4.6.



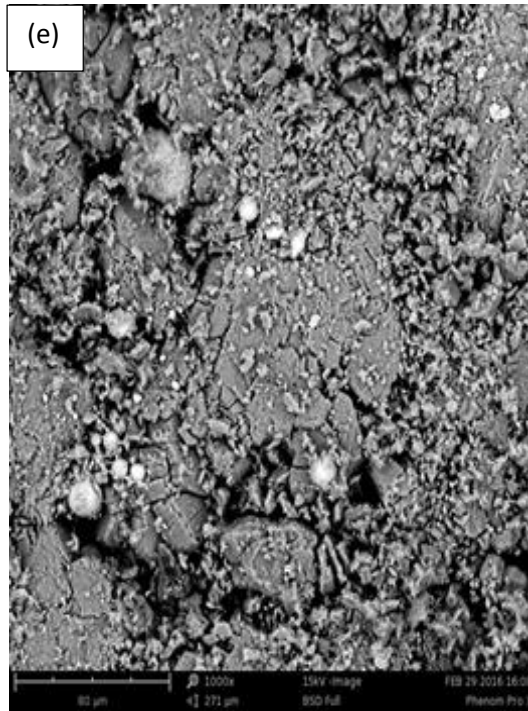


Figure 4.6: SEM micrographs of (a) 100%  $\text{Al}_2\text{O}_3$ , (b) 95%  $\text{Al}_2\text{O}_3$  with 5% Fe addition, (c) 90%  $\text{Al}_2\text{O}_3$  with 10% Fe addition, (d) 95%  $\text{Al}_2\text{O}_3$  with 5% Cu addition, (e) 90%  $\text{Al}_2\text{O}_3$  with 10% Cu addition

The microstructure of pure alumina is presented in Figure 4.6(a), which displays the alumina grey phase and porosity appears as black colour. With only alumina, there are pores found in the sintered sample and also confirmed in the SEM observation. Although the area of the pores is relatively small but most of them are interconnected, this is corresponding to the relatively low sintered density obtained (78.93%) in this sample.

From Figure 4.6(b), the microstructure of alumina composites with 5 vol.% of iron addition is presented. It is noted that the darker phase is alumina and lighter phase is iron. The iron additions are well dispersed in the alumina matrix and the amount of pores is reduced compared to pure alumina. No crack and delamination is found in the microstructure and the pores are much more isolated compared to pure alumina. This corresponds to the high flexural strength achieved, which almost doubled up the flexural strength of pure alumina.

However, at 10 vol.% of iron additions, slight agglomeration has been observed and presented in Figure 4.6(c). This can be the cause of relative density reduction from 82.77% at 5 vol.% to 80.69%. Besides, this also corresponds to the lower increment

rate of flexural strength compared to 5 vol.% of iron. This indicated that the alumina-iron composite is reaching the optimum volume of iron content.

From Figure 4.6(d), the SEM micrograph of 5 vol.% copper alumina-copper composite is much different with the other composites. There are plenty of continuous pores distributed throughout the structure, and the relative density was only 77.56%. The copper melted during the sintering process and leaving behind pores in the structure. It can be seen at the top part of Figure 4.6(d), the copper (lighter phase) filled the gaps between alumina (darker phase). However, at the bottom part of the micrograph, the copper still exists but not enough to fill the gaps. This led to a low flexural strength. The flexural strength of 5 vol.% copper addition to alumina is lower than pure alumina. The continuous pores can cause stress concentration and promotes crack initiation around the pores, this is a huge disadvantage to its flexural strength. Therefore, the flexural strength recorded is only 120.2MPa.

Based on Figure 4.6(e), it showed that copper dispersed well in the alumina matrix. Throughout the structure, most of the pores are isolated but there are still continuous pores. Although the percentage volume of copper added increased from 5% to 10%, the copper content still insufficient to fill the existing gaps. Besides the low copper content, wettability problem may also be the cause of this structure. With increment of copper content, the flexural strength of alumina-copper composites is 170.1MPa, which is much better than 5 vol.% of copper. This showed that alumina-copper composites required a relatively higher copper content in order to achieve high flexural strength. This is in line with the findings by Travitzky [4], who reported that alumina-copper composites with 15 vol.% copper able to achieve continuous alumina-cuprite network and flexural strength in the range of 335MPa to 375MPa.

#### **4.5 Optimum Volume of Iron or Copper Additions**

After determining the alumina-iron and alumina copper composites' density, flexural strength and microstructure, the data are combined in order to identify its optimum volume of metal additions. Figures 4.7 and 4.8 show the combined results of alumina-iron composites and alumina-copper composites respectively.



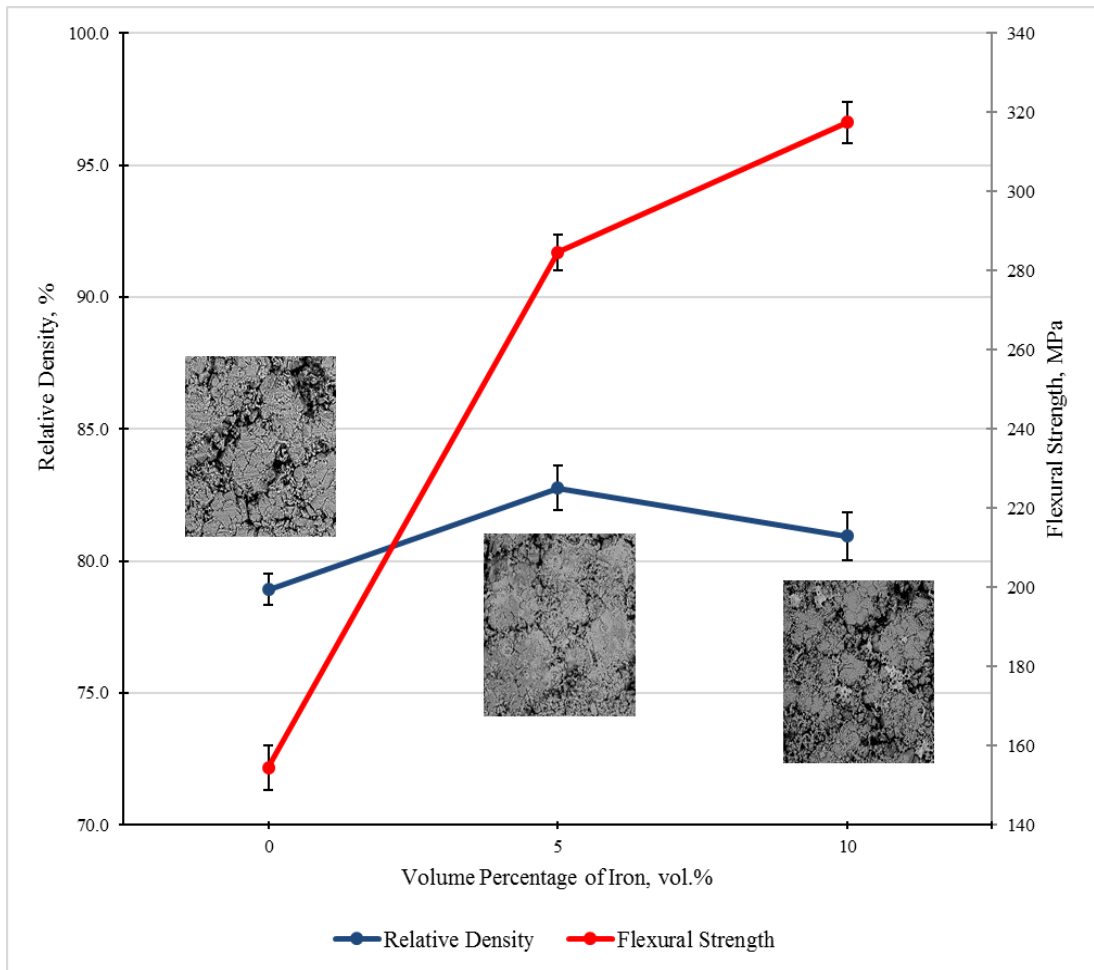


Figure 4.7: Combined Data of Alumina-iron Composites

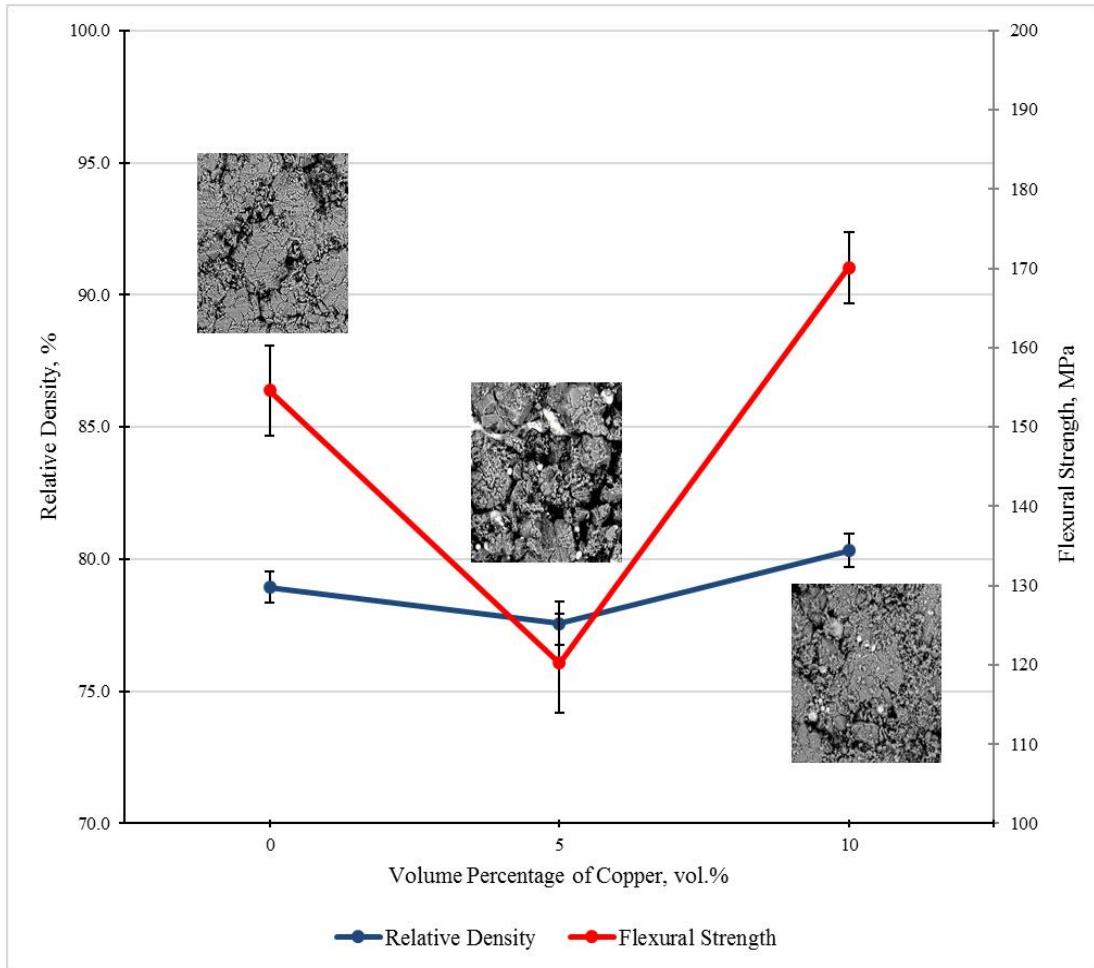


Figure 4.8: Combined Data of Alumina-copper Composites

Based on Figure 4.7, the optimum volume of iron addition to reinforce the mechanical properties of alumina is in the range of 5 vol.% to 10 vol.%. The iron able to incorporate its mechanical properties to the alumina-iron composites effectively at 5 vol.%; this is shown in the flexural strength recorded (284.6MPa). Further increment of iron content did improve its flexural strength, but at a lower rate. However, the iron started to agglomerate at 10 vol.%, this can be seen from the SEM micrographs obtained. It is believed that further increased the iron content will result in similar condition. Therefore, it is recommended to keep the iron content in alumina-iron composites within 5 vol.% to 10 vol.%.

For alumina-copper composites, the combined result is presented in Figure 4.8. Copper addition with less than 5 vol.% is definitely not an optimum volume. This is because the low volume of copper content leaving behind continuous pores after the sample is sintered at a sintering temperature which is higher than melting temperature of copper.

Furthermore, the low volume of copper failed to enhance the flexural strength of alumina. At 10 vol.% of copper content, there is less continuous pores compared to 5 vol.% but the copper volume can be further increased in order to achieve a homogenous structure. The flexural strength obtained is 170.1MPa, which is slightly higher than pure alumina. From the range of 0 vol.% to 10 vol.% of copper addition, the result recorded at 10 vol.% did improve the mechanical properties of pure alumina, although the improvement is not that significant. In this case, the optimum volume of copper addition to alumina-copper composites is at 10 vol. %.

## **CHAPTER 5 CONCLUSION AND RECOMMENDATIONS**

### **5.1 Conclusion**

In this study, alumina-iron and alumina-copper ceramic composites in 5 vol.% and 10 vol.% iron and copper content are fabricated by powder metallurgy. A total of 25 samples are produced and analysis in terms of density, flexural strength and microstructures of composites had been carried out successfully. The incorporation of metal into alumina increased the density of alumina. All the alumina based composites samples with various compositions have higher density compared to pure alumina. With 10 vol.% of iron addition, it doubled the flexural strength of pure alumina, whereas for copper addition, the improvement in flexural strength is less significant. The microstructural analysis revealed the microstructure conditions for both type of composites with different composition. The flexural strength achieved by composites are related to their respective microstructural properties. From the combined data of relative density, flexural strength and microstructures, the optimum values of metal additions are determined. For alumina-iron composite, the optimum iron content to enhance flexural strength is in the range of 5 vol.% to 10 vol.%; whereas for alumina-copper composite, the optimum copper content is at 10 vol.%.

### **5.2 Recommendations**

Below are the suggestions provided in improving this study and for future works.

i. Samples fabrication method

About the fabrication of samples, uniaxial press can be replaced by hot isostatic press in producing green compacts. This helps in increasing the green density, and thus the sintered density will be closer to the theoretical value. With higher quality samples, it is believed that the accuracy of results will be improved.

ii. Range of metal content in alumina-metal composites

Due to time constraint, the alumina-iron and alumina-copper composites prepared are limited to 5 vol.% and 10 vol.% of metal additions. For future expansion, it is recommended to increase the range of volume percentage of iron and copper additions in alumina based composites. This can further analyse the trend of mechanical properties with respect to wider composition range of alumina-metal composites.

## REFERENCES

- [1] Z. He, J. Ma, and G. E. B. Tan, "Fabrication and characteristics of alumina–iron functionally graded materials," *Journal of Alloys and Compounds*, vol. 486, (1-2), pp. 815-818, 2009.
- [2] S. A. Brent, "Ceramic and metal matrix composites," in *Fundamentals of Composites Manufacturing - Materials, Methods, and Applications*, 2nd. ed., Michigan: Society of Manufacturing Engineers, 2008, pp. 179-195.
- [3] W. D. Callister and D. G. Rethwisch, *Materials Science and Engineering*, 8th. ed., New Jersey: John Wiley & Sons, 2009.
- [4] N. A. Travitzky, "Microstructure and mechanical properties of alumina/copper composites fabricated by different infiltration techniques," *Materials Letters*, vol. 36, (1-4), pp. 114-117, 1998.
- [5] A. K. Kaw, "Introduction to composite materials," in *Mechanics of Composite Materials*, 2nd. ed., Boca Raton: CRC Press, 2006, pp. 1-54.
- [6] I. M. Low, "Introduction" in *Ceramic-Matrix Composites Microstructures, Properties and Applications*, Cambridge: Woodhead Publishing, 2006, pp. 1-6.
- [7] Z. Yin, C. Huang, B. Zou, H. Liu, H. Zhu, and J. Wang, "Effects of particulate metallic phase on microstructure and mechanical properties of carbide reinforced alumina ceramic tool materials," *Ceramics International*, vol. 40, pp. 2809-2817, 2014.
- [8] E. P. Chassale, E. R. Rangel and M. R. Romo. "Production, microstructural comparison and mechanical behaviour of reinforced alumina composites containing zirconia, silicon carbide, nickel and titanium," *Journal of Ceramic Processing Research*, vol. 11(3), pp. 372-376, 2010.
- [9] J. O. Ramos, E. R. Garcia, E. T. Rojas, J. G. M. Hernandez, J. A. R. Garcia, and E. R. Rangel, "Alumina based composite reinforced with ductile particles," *International Journal of Research in Engineering and Science*, vol. 2(6), pp. 60-64, 2014.
- [10] R. I Made, E. J. R. Phua, S. S. Pramana, C. C. Wong, Z. Chen, A. I. Y. Tok, *et al.*, "Improved mechanical and thermomechanical properties of alumina substrate via iron doping," *Scripta Materialia*, vol. 68, pp. 869-872, 2013.
- [11] J. G. M. Hernández, A. B. S. Guzman and E. R. Rangel, "Production and characterization of Al<sub>2</sub>O<sub>3</sub>-Cu composite materials." *Journal of Ceramic Processing Research*, vol. 7(4), pp. 311-314, 2006.

- [12] W. Soboyejo, "Introduction to composites," in *Mechanical Properties of Engineered Materials*, New York: Marcel Dekker Inc, 2003, pp. 248-287.
- [13] P. Auerkari, "*Mechanical and Physical Properties of Engineering Alumina Ceramics*," Finland: Technical Research Centre of Finland VTT, 1996.
- [14] L. F. Pease and W. G. West, "Visual basics - A quick tour of powder metallurgy," in *Fundamentals of Powder Metallurgy*, New Jersey: Metal Powder Industries Federation, 2002, pp. 51-69.
- [15] J. S. Winzer, "*Production and Characterization of Alumina-copper Interpenetrating Composites*," Giessen: VVB Laufersweiler Verlag, 2011.
- [16] P. C. Angelo and R. Subramanian, "Production of powders," in *Powder Metallurgy Science, Technology and Applications*, New Delhi: PHI Learning Private Limited, 2008, pp. 19-40.
- [17] R. M. German, *Powder Metallurgy Science*, 2nd, ed., United States of America: The Pennsylvania State University, 1997.
- [18] J. Cho, A. Boccaccini, and M. P. Shaffer, "Ceramic matrix composites containing carbon nanotubes," *Journal of Material Science*, vol. 44, (8), pp. 1934-1951, 2009.
- [19] S. Kalpakjian and S. Schmid, "Processing of metal powders," in *Manufacturing, Engineering and Technology*, 5th. ed., Singapore: Pearson Education, 2006, pp. 437-464.
- [20] L. C. De Jonghe and M. N. Rahaman, "4.1 Sintering of ceramics," in *Handbook of Advanced Ceramics*, Oxford: Academic Press, 2003, pp. 187-264.
- [21] K. Biswas, "Liquid phase sintering of SiC-ceramics," *Materials Science Forum*, vol. 624, pp.91-108, 2009.
- [22] M. Rahimian, N. Parvin, and N. Ehsani, "Investigation of particle size and amount of alumina on microstructure and mechanical properties of Al matrix composite made by powder metallurgy," *Materials Science and Engineering: A*, vol. 527, (4-5), pp. 1031-1038, 2010.
- [23] S. J. E. Vazquez, E. R. Rangel, J. A. R. Garcia, and C. A. Hernandez-Bocanegra, "Strengthening of alumina-based ceramics with titanium nanoparticles," *Materials Sciences and Applications*, vol. 5, pp. 467-474, 2014.
- [24] T. Tani, "Processing, microstructure and properties of in-situ reinforced SiC matrix composites," *Composites Part A: Applied Science and Manufacturing*, vol. 30, (4), pp 419-423, 1999
- [25] M. Rahimian, N. Ehsani, N. Parvin, and H.R. Baharvandi, "The effect of particle size, sintering temperature and sintering time on the properties of Al–Al<sub>2</sub>O<sub>3</sub>

composites, made by powder metallurgy," *Journal of Materials Processing Technology*, vol. 209, (14), pp. 5387-5393, 2009.

- [26] J. Winzer, L. Weiler, J. Pouquet, and J. Rödel, "Wear behaviour of interpenetrating alumina–copper composites," *Wear*, vol. 271, pp. 2845-2851, 2011.
- [27] H. J. Kim, S. M. Lee, Y. S. Oh, Y. H. Yang, Y. S. Lim, D. H. Yoon, et al., "Unoxidized graphene/alumina nanocomposite: fracture and wear resistance effects of graphene on alumina matrix," *Scientific Reports*, vol. 4, pp. 5176-5185, 2014.
- [28] K. Ahmad and W. Pan, "Microstructure-toughening relation in alumina based multiwall carbon nanotube ceramic composites," *Journal of European Ceramic Society*, vol. 35, pp. 663-671, 2015.

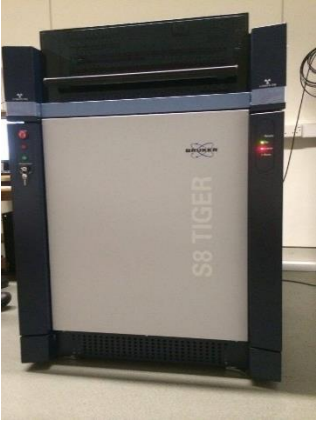
**APPENDIX A – Table of engineering alumina grades A1- A9 and their characteristics at room temperature**





Table I: Engineering alumina grades A1- A9 and their characteristics at room temperature [13]

Grade	Al <sub>2</sub> O <sub>3</sub> , min %	Porosity, %	Density, g/cm <sup>3</sup>	Young's Modulus, GPa	Avg. Compressive Strength, MPa	Hardness, HV 1.0
A1	99.6	0.2-3	3.75-3.95	410-380	>4000	1500-2000
A2	99.8	<1	3.97-3.99	405-380	>4000	1500-9000
A3	99.5	<1	3.90-3.99	400-398	>3000	NA
A4	99.6	3-6	3.75-3.85	380-340	>4000	NA
A5	99.0	1-5	3.76-3.94	380-340	>4000	1300-1700
A6	96.5- 99.0	2-5	3.71-3.92	375-340	>3000	1200-1600
A7	94.5- 96.5	2-5	3.60-3.90	370-300	>3000	1200-1400
A8	86.0- 94.5	2-5	3.40-3.90	330-260	>2500	900-1200
A9	80.0- 86.0	3-6	3.30-3.60	330-260	>2000	800-1000



## APPENDIX B – Equipment needed

No.	Equipment	Photo
1	Mettler Toledo digital weighing scale	 A photograph of a white Mettler Toledo digital weighing scale. The scale has a large, clear protective cover that is currently open, revealing the weighing pan and the internal mechanism. The text "BALANCE MAX 200G" is visible on the top of the cover. The scale's control panel features a small LCD screen and several buttons.
2	XRF spectrometer	 A photograph of a large, industrial-grade X-ray fluorescence (XRF) spectrometer. The machine is primarily black with a prominent silver-colored front panel. The text "S8 TIGER" is printed vertically on the silver panel. The device has a complex, boxy design with various ports and a control interface on the left side.
3	Tubular mixer	 A photograph of a laboratory tubular mixer. The mixer is housed in a clear, rectangular plastic enclosure. Inside, a blue, cylindrical mixing chamber is visible, equipped with internal mixing blades. A label on the front of the enclosure reads "L'ECOLE NATIONALE DES TUBULAIRES". The mixer is placed on a dark surface.

4	Compression machine	
5	Sintering furnace	
6	Scanning electron microscope	
7	Universal testing machine	

## APPENDIX C – Sample calculations for mass of sample

Below is the sample calculation of conversion of volume percentage to mass for alumina-copper ceramic composites with 95% alumina and 5% copper:

Alumina,

$$\begin{aligned} \text{Volume}_{\text{alumina}} &= V_{f_{\text{alumina}}} \times \text{Volume}_{\text{composite}} \\ &= 0.95 \times 2.56 \text{cm}^3 \\ &= 2.43 \text{cm}^3 \end{aligned}$$

$$\begin{aligned} \text{Mass}_{\text{alumina}} &= \text{Density}_{\text{alumina}} \times \text{Volume}_{\text{alumina}} \\ &= 3.75 \text{g/cm}^3 \times 2.43 \text{cm}^3 \\ &= 9.11 \text{g} \end{aligned}$$

Copper,

$$\begin{aligned} \text{Volume}_{\text{copper}} &= V_{f_{\text{copper}}} \times \text{Volume}_{\text{composite}} \\ &= 0.05 \times 2.56 \text{cm}^3 \\ &= 0.128 \text{cm}^3 \end{aligned}$$

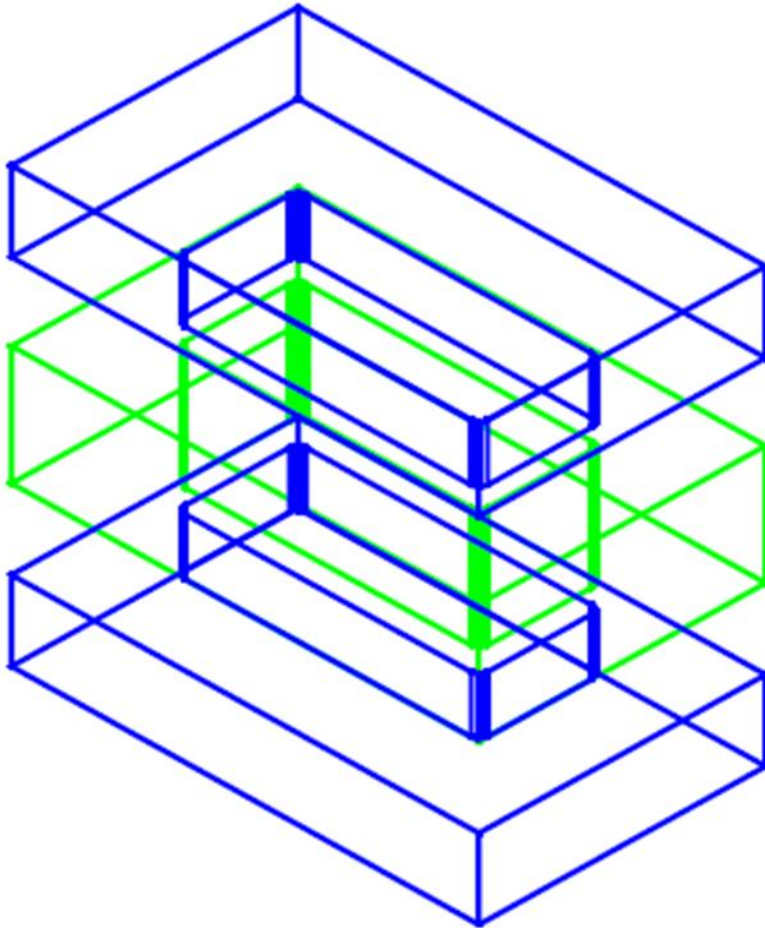
$$\begin{aligned} \text{Mass}_{\text{copper}} &= \text{Density}_{\text{copper}} \times \text{Volume}_{\text{copper}} \\ &= 8.94 \text{g/cm}^3 \times 0.128 \text{cm}^3 \\ &= 1.14 \text{g} \end{aligned}$$

Total mass for alumina-copper ceramic composites with 95% alumina and 5% copper,

$$\begin{aligned} \text{Mass}_{\text{composite}} &= \text{Mass}_{\text{alumina}} + \text{Mass}_{\text{copper}} \\ &= 9.11 \text{g} + 1.14 \text{g} \\ &= 10.25 \text{g} \end{aligned}$$

## APPENDIX D1 – Mould design for compaction process

Below is a through-hole mould with top and bottom punch in SE isometric view designed using AutoCAD. The total height of the mould is 67.4mm. The width and length of mould are 35mm and 60mm respectively.

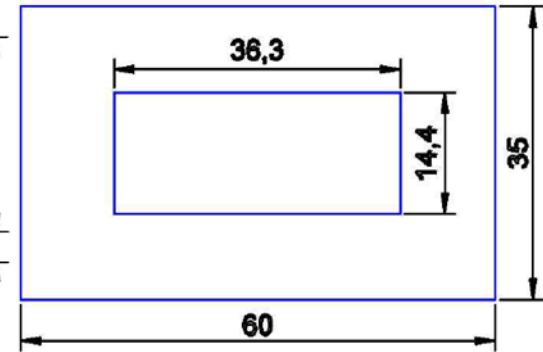
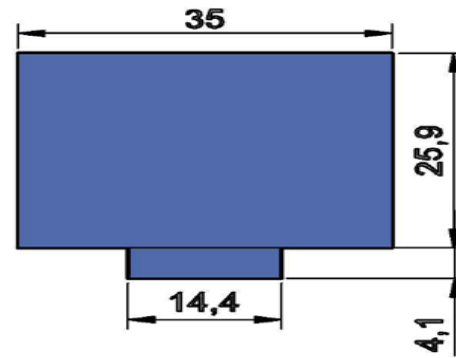
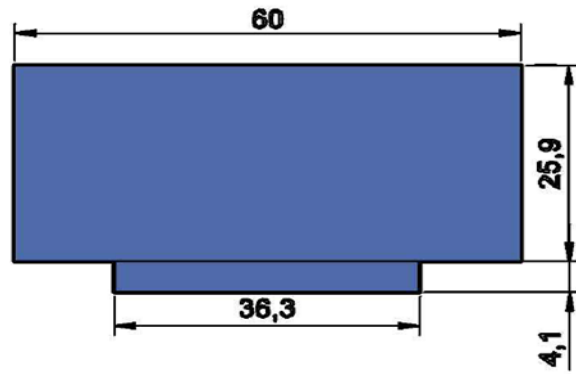


**APPENDIX D2 – Mould dimensions**

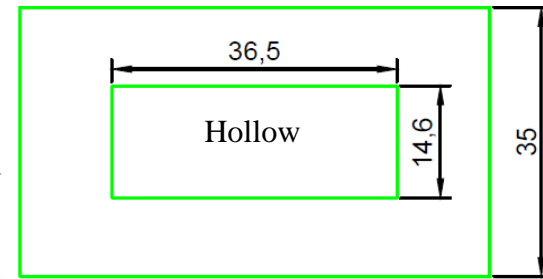
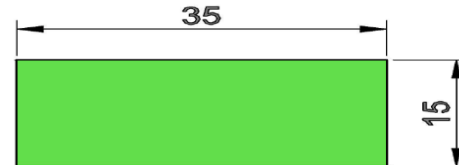
Side view

Top view

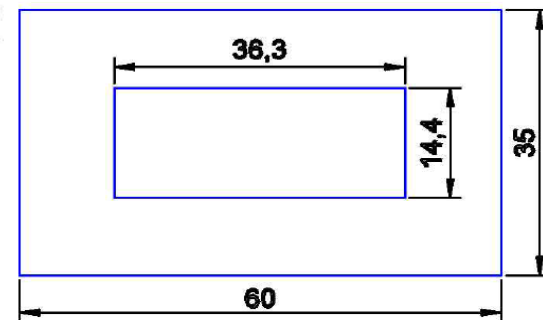
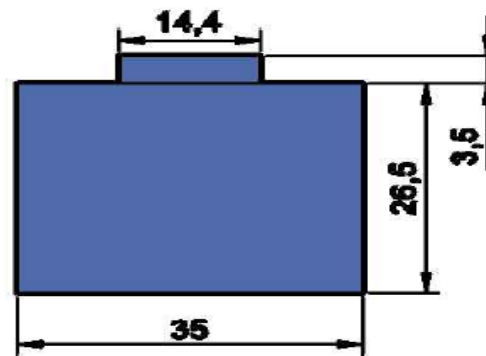
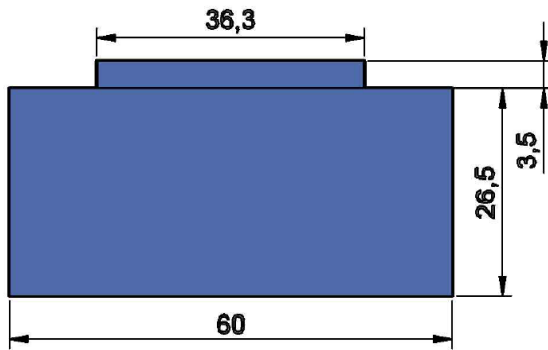
Top punch  
(Male)



Female part



Bottom punch  
(Male)



## APPENDIX E – XRF analysis results for alumina, iron and copper powder

### Alumina

Concentration	Formula	z	Status	Line 1	Stat error.	Net int	Calc. concentration	LLD	Analyzed Layer
95.6 %	Al	13	XRF 1	Al KA1-HR-Tr	0.417 %	184.8	95.57	132.2 PPM	13.7µm
2.92 %	P	15	XRF 1	P KA1-HR-Tr	2.88 %	4.148	2.92	126.5 PPM	2.83µm
1.20 %	Ca	20	XRF 1	Ca KA1-HR-Tr	3.01 %	3.753	1.20	58.8 PPM	13.5µm
0.153 %	Fe	26	XRF 1	Fe KA1-HR-Tr	4.52 %	3.071	0.153	32.3 PPM	62µm
0.0862 %	Ga	31	XRF 1	Ga KA1-HR-Tr	3.78 %	6.156	0.0861	19.3 PPM	178µm
0.0236 %	Cu	29	XRF 1	Cu KA1-HR-Tr	14.5 %	1.107	0.024	21.2 PPM	119µm
0.0228 %	Zn	30	XRF 1	Zn KA1-HR-Tr	13.4 %	1.365	0.023	19.1 PPM	146µm
0.0202 %	Ni	28	XRF 1	Ni KA1-HR-Tr	18.5 %	0.7389	0.020	23.2 PPM	96µm

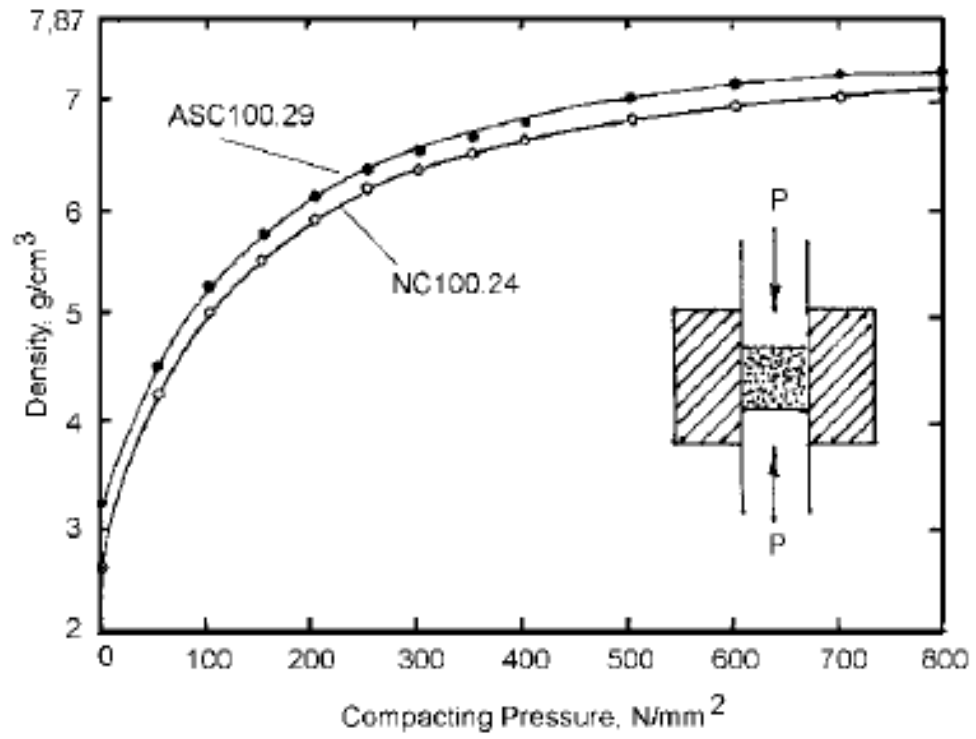
### Iron

Concentration	Formula	z	Status	Line 1	Stat error.	Net int	Calc. concentration	LLD	Analyzed Layer
99.5 %	Fe	26	XRF 2	Fe KA1-HR-Tr	0.0580 %	9529	103.9	199.1 PPM	29.9µm
0.327 %	P	15	XRF 1	P KA1-HR-Tr	2.83 %	4.440	0.327	117.2 PPM	1.31µm
0.111 %	Ca	20	XRF 1	Ca KA1-HR-Tr	3.23 %	3.806	0.111	73.8 PPM	6.6µm
0.0410 %	Cl	17	XRF 1	Cl KA1-HR-Tr	10.2 %	0.7421	0.041	137.5 PPM	2.62µm
0.0185 %	Rh	45	XRF 1	Rh KA1-HR-Tr	17.5 %	0.2135	0.019	109.3 PPM	86µm

### Copper

Concentration	Formula	z	Status	Line 1	Stat error.	Net int	Calc. concentration	LLD	Analyzed Layer
99.3 %	Cu	29	XRF 2	Cu KA1-HR-Tr	0.0422 %	17952	114.5	183.6 PPM	36µm
0.438 %	P	15	XRF 1	P KA1-HR-Tr	2.81 %	4.454	0.438	148.3 PPM	0.87µm
0.160 %	Ca	20	XRF 1	Ca KA1-HR-Tr	3.09 %	3.988	0.160	91.6 PPM	4.3µm
0.0316 %	Si	14	XRF 1	Si KA1-HR-Tr	20.2 %	0.1710	0.032	178.2 PPM	0.60µm
0.0226 %	S	16	XRF 1	S KA1-HR-Tr	13.7 %	0.4675	0.023	103.5 PPM	1.23µm
0.0194 %	Ni	28	XRF 1	Ni KA1-HR-Tr	6.26 %	3.135	0.019	48.9 PPM	29.7µm
0.0284 %	Fe	26	XRF 1	Fe KA1-HR-Tr	10.8 %	1.389	0.008	34.9 PPM	19.3µm

**APPENDIX F – Graph of density against compaction pressure for iron**



## APPENDIX G – Sintered samples

Composition	Sintered Samples
100% Al <sub>2</sub> O <sub>3</sub>	 Five light-colored, rectangular sintered samples of 100% Al <sub>2</sub> O <sub>3</sub> are shown in a row. Below them is a ruler with two scales: the top scale is in centimeters (0 to 11) and the bottom scale is in millimeters (0 to 15).
95% Al <sub>2</sub> O <sub>3</sub> – 5% Fe	 Five greyish-green, rectangular sintered samples of 95% Al <sub>2</sub> O <sub>3</sub> – 5% Fe are shown in a row. Below them is a ruler with two scales: the top scale is in centimeters (0 to 10) and the bottom scale is in millimeters (0 to 15).
90% Al <sub>2</sub> O <sub>3</sub> – 10% Fe	 Five dark grey, rectangular sintered samples of 90% Al <sub>2</sub> O <sub>3</sub> – 10% Fe are shown in a row. Below them is a ruler with two scales: the top scale is in centimeters (0 to 11) and the bottom scale is in millimeters (0 to 15).



95%  $\text{Al}_2\text{O}_3$  – 5% Cu



90%  $\text{Al}_2\text{O}_3$  – 10% Cu



**APPENDIX H1 – Mass, volume and density of green compacts**

<b>Sample Composition</b>	<b>Mass, g</b>	<b>Volume, cm<sup>3</sup></b>	<b>Green Density, g/cm<sup>3</sup></b>
100% Al <sub>2</sub> O <sub>3</sub>	9.71	3.74	2.59
	9.63	3.70	2.60
	9.66	3.82	2.53
	9.57	3.62	2.64
	9.53	3.74	2.49
95% Al <sub>2</sub> O <sub>3</sub> – 5% Fe	10.22	3.70	2.76
	10.28	3.82	2.69
	10.32	3.74	2.76
	10.17	3.74	2.72
	10.11	3.78	2.67
90% Al <sub>2</sub> O <sub>3</sub> – 10% Fe	10.73	3.86	2.78
	10.66	3.82	2.79
	10.61	3.74	2.83
	10.53	3.82	2.75
	10.57	3.81	2.76
95% Al <sub>2</sub> O <sub>3</sub> – 5% Cu	10.27	3.82	2.67
	10.22	3.82	2.67
	10.18	3.74	2.72
	10.26	3.82	2.68
	10.13	3.78	2.68
90% Al <sub>2</sub> O <sub>3</sub> – 10% Cu	11.00	3.78	2.91
	11.03	3.82	2.88
	11.15	3.91	2.86
	10.85	3.86	2.81
	11.01	3.82	2.88

**APPENDIX H2 – Mass, volume and density of sintered samples**

<b>Sample Composition</b>	<b>Mass, g</b>	<b>Volume, cm<sup>3</sup></b>	<b>Sintered Density, g/cm<sup>3</sup></b>
100% Al <sub>2</sub> O <sub>3</sub>	9.71	3.22	3.01
	9.63	3.26	2.95
	9.66	3.22	3.00
	9.57	3.30	2.90
	9.53	3.26	2.92
95% Al <sub>2</sub> O <sub>3</sub> – 5% Fe	10.22	3.14	3.25
	10.28	3.10	3.32
	10.32	3.22	3.20
	10.17	3.26	3.12
	10.11	3.14	3.22
90% Al <sub>2</sub> O <sub>3</sub> – 10% Fe	10.73	3.22	3.33
	10.66	3.18	3.35
	10.61	3.30	3.21
	10.53	3.34	3.15
	10.57	3.22	3.28
95% Al <sub>2</sub> O <sub>3</sub> – 5% Cu	10.23	3.22	3.18
	10.22	3.30	3.10
	10.18	3.22	3.16
	10.26	3.26	3.14
	10.13	3.38	3.00
90% Al <sub>2</sub> O <sub>3</sub> – 10% Cu	11.00	3.18	3.46
	11.03	3.18	3.47
	11.15	3.22	3.46
	10.85	3.26	3.33
	11.01	3.18	3.46